Competition for a limited pool of cohesin between centromeres and the rDNA triggers chromosomal instability that shortens replicative lifespan

Ryan D. Fine[1], Nazif Maqani[1], Mingguang Li[1,2], Elizabeth Franck[1], and Jeffrey S. Smith[1,*]

[1]Department of Biochemistry and Molecular Genetics, University of Virginia School of Medicine, Charlottesville, VA 22908. [2]Department of Laboratory Medicine, Jilin Medical University, Jilin, 132013, China

[*]Corresponding Author
Department of Biochemistry and Molecular Genetics
University of Virginia School of Medicine
Pinn Hall, Box 800733
Charlottesville, VA 22908

Phone: 434-243-5864
Fax: 434-924-5069
Email: jss5y@virginia.edu

Keywords: Sir2, Hst1, Mcd1, cohesin, Net1, RENT, Lrs4, monopolin, replicative lifespan, chromosome instability, rDNA, aging

Abstract

Sir2 is a highly conserved NAD^+-dependent histone deacetylase that functions in heterochromatin formation and promotes replicative lifespan (RLS) in the budding yeast, *Saccharomyces cerevisiae*. Within the yeast rDNA locus, Sir2 is required for efficient cohesin recruitment and maintaining stability of the tandem array. In addition to the rDNA, ChIP-seq of an epitope-tagged cohesin subunit (Mcd1-13xMyc) in a *sir2*Δ mutant revealed subtle reductions of cohesin binding at all 16 centromeres. Coupled with the previously reported chromosome instability in *sir2*Δ cells and depletion of Sir2 in aged cells, we hypothesized that mitotic chromosome instability (CIN) due to Sir2 depletion could be a driver of replicative aging. In addition to Sir2, we discovered that other subunits of the Sir2-containing SIR and RENT complexes were depleted in aged cells, as were subunits of the cohesin and monopolin/cohibin complexes, implying the possibility of CIN. ChIP assays of the residual Mcd1-13xMyc in aged cells showed strong depletion from the rDNA and possible redistribution to centromeres, most likely in an attempt to maintain chromosome stability. Despite the shift in cohesin distribution, sister chromatid cohesion was partially attenuated in old cells and the frequency of chromosome loss was increased. This age-induced CIN was exacerbated in strains lacking Sir2 and its paralog, Hst1, but suppressed in strains that stabilize the rDNA array due to the deletion of *FOB1* or through caloric restriction (CR). Furthermore, ectopic expression of *MCD1* from a doxycycline-inducible promoter was sufficient to suppress to rDNA instability in aged cells and to extend RLS. Taken together we conclude that age-induced depletion of cohesin and multiple other nucleolar chromatin factors destabilize the rDNA locus, which then results in general CIN and aneuploidy that shortens RLS.

Author summary

The aging process is generally characterized by the breakdown of multiple cellular processes, including the maintenance of genome integrity. Alterations from the normal chromosome number is known as aneuploidy, and commonly occurs in oocytes (eggs) of older mothers. The risk of aneuploidy increases with age and can cause diseases such as Down's syndrome (chromosome 21 trisomy). It is therefore important to understand how aging causes the chromosome instability (CIN) that leads to aneuploidy. In this study we have investigated whether CIN is associated with aging of mitotic cells using the budding yeast, *Saccharomyces cerevisiae*, as a model system. We show that chromosomes are indeed lost during aging of these cells due to the depletion of several key proteins that function in organizing and maintaining chromosome architecture, including the cohesin complex. Restoring cohesin levels was sufficient to delay aging, and adding extra cohesin even extended normal lifespan. Lastly, caloric restriction (CR), a dietary modification known to extend lifespan of yeast and other model organisms, strongly prevented chromosome instability, suggesting a possible new mechanism for how CR delays age-associated conditions at the cellular level.

Introduction

Budding yeast replicative lifespan (RLS) was originally described decades ago as the number of times a mother cell divides before losing viability [1], and has been an effective model system for the identification and/or characterization of several conserved aging-related genes and pathways, including *SIR2*, AMPK (Snf1), and TOR signaling [2]. *SIR2* is probably the most famous yeast gene associated with replicative aging and encodes the founding family member of the NAD^+-dependent histone/protein deacetylases, commonly known as sirtuins (reviewed in [3]). The NAD^+ dependence of sirtuins provides a direct link between metabolism and cellular processes regulated by these enzymes. In fact, recent evidence points to depletion of cellular NAD^+ pools as a potential mechanism for aging-associated disease, which could be mediated by impairment of sirtuins or other NAD^+ consuming enzymes [4]. Therefore, understanding how sirtuins are impacted by aging and determining how they contribute to the regulation of age-altered cellular processes is of intense interest in the aging field.

Eukaryotic genomes generally encode for several different sirtuin homologs. The *Saccharomyces cerevisiae* genome, for example, encodes *SIR2* and four additional Homologs of Sir Two (*HST1-HST4*) [5]. Sir2 was originally shown to establish and maintain silencing of the silent mating loci, *HML* and *HMR*, along with its fellow Silent Information Regulator (SIR) proteins, Sir1, Sir3, and Sir4 [6]. Additionally, Sir2, Sir3, and Sir4 form the so-called SIR complex that is recruited to and then spreads across the *HM* loci and telomeres to form hypoacetylated heterochromatin-like domains (reviewed in [7]). Sir2 protein levels are significantly reduced in replicatively old yeast cells [8], presenting a possible mechanism for the decline of Sir2-dependent processes during aging, including gene silencing. Indeed, depletion of Sir2 in old cells causes hyperacetylated H4K16 and silencing defects at subtelomeric loci [8].

Haploid cells lacking Sir2 derepress *HML* and *HMR*, resulting in co-expression of mating type regulatory genes that together induce a diploid-like gene expression pattern that produces a non-mating "pseudodiploid" phenotype [6]. Old haploid mother cells are sterile, presumably due to the pseudodiploid effect [9], but more recent experiments point toward a silencing-independent mechanism caused by aggregation of the Whi3 protein and loss of pheromone sensitivity [10].

Alternative models for Sir2 control of RLS have focused on the rDNA tandem array. Sir2 functions in the silencing of RNA polymerase II-dependent transcription at the rDNA locus on chromosome XII via a nucleolar complex called RENT [11, 12], which consists of Sir2, Net1, and Cdc14 [13, 14]. RENT-dependent H3 and H4 deacetylation represses transcription of endogenous non-coding RNAs from the intergenic spacer (IGS) regions [15]. Derepression of the bidirectional promoter (E-pro) within IGS1 of *sir2*Δ cells displaces cohesin from the rDNA, thus destabilizing the array by making it more susceptible to unequal sister chromatid exchange [16]. A predominant model for *SIR2* control of replicative aging postulates that extrachromosomal rDNA circles (ERCs) derived from these unequal recombination events specifically accumulate to high levels in mother cells, consequently causing cell death through an unknown mechanism [17]. Such an ERC-centric model is supported by the extended RLS extension of *fob1*Δ strains [18]. Fob1 binds to the rDNA in IGS1 to block DNA replication forks from colliding with RNA polymerase I transcribing in the opposite direction [19]. The blocked replication forks can collapse and result in double-stranded DNA breaks that trigger the unequal sister chromatid exchange [20]. The frequency of rDNA recombination and ERC accumulation is significantly reduced in a *fob1*Δ mutant due to loss of the fork block, thus extending RLS [18]. This rDNA-centric model of replicative aging has been modified over the years such that overall rDNA instability, rather than ERC accumulation, is now considered the critical deleterious factor

toward lifespan [21]. Strains with virtually no ERC accumulation in old cells, but a high frequency of rDNA recombination, are short-lived [22]. Also consistent with this idea, *sir2*Δ still reduces RLS in a *fob1*Δ strain that has limited ERCs [23]. This raises several important questions, including 1) does Sir2 regulate RLS through mechanisms independent of the rDNA, and 2) how does rDNA instability shorten RLS? The experiments in this current study address both of these questions.

As mentioned above, Sir2 is required for efficient cohesin association with the rDNA, with stabilization of the tandem array a major mechanism for maintaining replicative longevity. The cohesin complex in *S. cerevisiae* consists of four subunits, Mcd1/Scc1, Irr1/Scc3, Smc1, and Smc3 [24]. The cohesin loading complex (Scc2/Scc4) deposits cohesin onto centromeres and other sites across the chromosome arms (including rDNA) during S-phase to maintain sister chromatid cohesion (SCC) until anaphase, when the Mcd1 subunit is cleaved by separase to facilitate sister chromatid separation (reviewed in [24]). Cohesin defects result in chromosome instability (CIN) and aneuploidy due to improper chromosome segregation during mitosis (reviewed in [25]. Interestingly, cells lacking *SIR2* or heavily overexpressing *SIR2* have increased rates of chromosome loss [26, 27]. Aneuploidy has been shown to shorten yeast RLS by inducing proteotoxicity through improper expression levels [28]. Taken together, these results suggest that Sir2 could impact RLS by regulating mitotic chromosome segregation during aging.

In this study, we investigated a potentially novel role for Sir2-limited yeast RLS through maintenance of accurate chromosome segregation. In the process, we uncovered chromosome instability and SCC defects in aging yeast cells that correlated with reduced levels of cohesin and cohesin loader subunits. Forcibly manipulating Mcd1 subunit levels was sufficient to modify RLS, suggesting a causative relationship to aging. Interestingly, cohesin association with

chromosome arms and the rDNA was generally reduced in old cells, but maintained or even increased at centromeres, suggesting a programmed mechanism by which SCC is preferentially maintained at centromeres to ensure cell viability. However, this comes at the expense of chronic rDNA instability that is exacerbated by age-induced reductions in the RENT and cohibin/monopolin complexes. Lastly, reducing rDNA instability by deleting *FOB1* suppressed the general CIN phenotype in aged cells, leading to a model whereby rDNA instability caused by cohesin depletion drives the defects in mitotic segregation of other chromosomes during replicative aging.

Results

We previously reported a statistically significant overlap in genome-wide Sir2 binding sites measured by ChIP-seq with cohesin binding sites measured by ChIP-Chip microarray analysis [29, 30], consistent with the idea of a functional relationship between the two. Since deleting *SIR2* reduced cohesin recruitment at individually selected loci [30], including the rDNA [31], we decided to explore this result further using ChIP-Seq with exponentially growing WT and *sir2*Δ strains in which the Mcd1 subunit of cohesin was C-terminally tagged with 13 copies of the myc epitope (13xMyc). A composite plot of the sequencing data normalized to 1X read coverage indicated both replicates of the *sir2*Δ strain exhibited dramatically reduced levels of Mcd1-myc binding within the rDNA locus as compared to the WT strain (Fig 1A). This result was confirmed with ChIP-qPCR using an IGS1 primer pair (Fig 1B) and supported earlier ChIP results from the Nomura lab showing that cohesin recruitment to the rDNA requires Sir2 [31]. It was also reported that cohesin released from the rDNA in a *sir2*Δ mutant preferentially relocalized to pericentromeric regions as measured by fluorescence microscopy of GFP-tagged

Smc3 [32]. We attempted to recapitulate this result by creating a composite profile of all 16 centromeres but did not detect the same pericentromeric enrichment of Mcd1-myc in our *sir2*Δ ChIP-seq datasets (Fig 1C). There was instead a trend toward reduced cohesion association. Standard ChIP assays also did not reveal evidence of significant centromeric or pericentromeric enrichment (Fig 1D). However, we cannot rule out the possibility that the ChIP signal was diluted within an asynchronous cell population, compared to the microscopy data that examined mitotic cells.

Cohesin levels are depleted in old yeast cells

Strains deleted for *SIR2* are short lived, but they likely do not fully recapitulate all cellular changes that accompany normal replicative aging. We therefore hypothesized that more severe effects of cohesin localization at centromeres could be uncovered by comparing replicatively young vs. old cells in which Sir2 protein levels naturally declined. To isolate sufficient quantities of old cells for ChIP assays we turned to Mother Enrichment Program (MEP) strains developed by the Gottschling lab [33]. The aged cell purification procedure was validated by increased bud scar staining with calcofluor white and by the expected reduction of Sir2 protein (Fig 2A). The vacuolar protein Vma2, used as a loading control, does not deplete with age [34], and detailed bud scar and protein quantitation from triplicate biological samples are reported in S1 Fig. Since Sir2 is the catalytic subunit of both SIR and RENT (Fig 2B), it was important to know which complexes were impacted by age. As shown in Figs 2C and 2D, Sir4 was depleted in old cells while Sir3 was not. Such a stark difference was considered highly relevant because Sir2 and Sir4 tightly interact as a heterodimer that associates with the acetylated H4 N-terminal tail [35]. Sir3 is subsequently recruited following H4K16 deacetylation to

complete SIR holocomplex formation on heterochromatin [36]. Myc-tagged Net1 (RENT complex) was also depleted from old cells (Fig 2E), indicating that Sir2/Sir4 and the RENT complex are both depleted during replicative aging, thus revealing a previously unrecognized level of specificity in age-related Sir2 protein homeostasis. It should be noted that the Sir2 paralog, Hst1, which has the capacity to compensate for loss of Sir2, is also partially depleted from old cells (S2A Fig).

Considering the depletion of multiple heterochromatin factors in old yeast cells and the generally reduced Mcd1-myc ChIP signal in *sir2*Δ cells, we hypothesized that cohesin complex levels may also drop in old cells. We attempted to individually myc-tag three different subunits of cohesin (Mcd1, Smc1, and Irr1) in the MEP strain background. All cohesin subunits are essential, and only two of the tagged proteins (Mcd1 and Smc1) were functional based on recovery of viable cells and proper size on western blots. Both of these subunits were significantly depleted in old cells (Fig 2F and S2B Fig), indicating the entire cohesion complex was affected. Furthermore, a Myc-tagged Scc2 subunit of the Scc2/Scc4 cohesin loading complex was age-depleted (S2C Fig), predicting that cohesion complex association with chromatin should be generally sparse. ChIP assays for Mcd1-myc in aged cells did demonstrate strong depletion from the rDNA intergenic spacer IGS1 as expected, but binding was surprisingly enhanced at the centromere of chromosome IV (Fig 2G). Sir4-myc, on the other hand, was depleted from *TELXV* in old cells (one of its normal targets) without shifting its enrichment to centromeres (*CEN4*) or the rDNA (Fig 2H), indicating that not all age-depleted proteins become enriched at centromeres. From these results we conclude that as cohesin is depleted during replicative aging, a significant portion of the remaining complex is retained and potentially redistributed to centromeres, consistent with an earlier finding that cohesin

195 preferentially associates with pericentromeric regions instead of chromosome arms when Mcd1
196 expression is artificially reduced below 30% of normal [37].
197
198 **Sister chromatid cohesion is compromised in old yeast cells**
199 SCC was surprisingly normal despite artificially reduced Mcd1 levels [37], leading us to
200 ask whether cohesion would be maintained in old yeast cells that were also depleted of cohesin.
201 To this end, we utilized strains with LacO arrays located approximately 10 kb away from
202 centromere IV (*CEN4*) or on the arm of chromosome IV at the *LYS4* locus located approximately
203 400 kb away from the centromere as proxy for arm cohesion [38, 39]. Differential positioning of
204 the array had no significant impact on RLS (S3 Fig). SCC was monitored by LacI-GFP
205 appearing either as one dot in the case of maintained cohesion or two dots in the case of cohesion
206 loss. Using an *mcd1-1* temperature sensitive mutant as a positive control [40], we observed a
207 significant increase in two dots when cells were synchronized in mitosis with nocodazole and
208 shifted to 37°C (Fig 3A and B). WT cells were next biotinylated and aged for 24 hours, followed
209 by purification with magnetic streptavidin beads. The maximum bud scar count was 13, which
210 was roughly half the maximum lifespan for this strain as measured by RLS assay. There was a
211 trend toward lost centromere and arm cohesion in old cells (>5 bud scars) when cultures were
212 synchronized in mitosis with nocodazole (Fig 3C, D, and E). When cells were not arrested with
213 nocodazole and only large budded (mitotic) cells were analyzed, significant cohesion loss was
214 observed in old mother cells compared to young (Fig 3E and F). Therefore, the limited amount of
215 cohesin complex remaining in old cells is functional, but has difficulty maintaining SCC when
216 microtubules are naturally allowed to exert pulling force on centromeres.
217

Chromosome instability (CIN) increases during replicative aging

Based on the cohesion defect in aged yeast cells, we next asked if they also display elevated chromosome instability. Strains for this experiment have an artificial chromosome III bearing a suppressor tRNA gene, *SUP11* [41]. Loss of the chromosome prevents suppression of an ochre stop codon in *ADE2*, resulting in the classic *ade2* red colony phenotype. The frequency of nondisjunction events was measured by counting half-sectored red/white colonies from young and aged cell populations (Fig 4A). A *sir2*Δ mutant was included in the experiment because it was previously reported to increase CIN [26], as was an *hst1*Δ mutant because of its potential for functional overlap with Sir2 [42, 43]. Sectoring was elevated in young populations of *sir2*Δ and *hst1*Δ mutants, and additively elevated in a *sir2*Δ *hst1*Δ double mutant (Fig 4B, left panel). Interestingly, sectoring was even higher for aged populations of each strain, suggesting an independent age-associated factor was involved. We next tested whether the *sir2*Δ effect on sectoring was related to the pseudodiploid phenotype caused by derepression of the *HM* loci. This reporter strain background was *MAT*α, so we deleted *HMR* (chrIII 293170-294330) to eliminate the a1/a2 transcription factors, and then confirmed reversal of the pseudodiploid phenotype by restoration of mating to the *sir2*Δ *hmr*Δ strains (data not shown). Importantly, this procedure significantly suppressed sectoring of the young *sir2*Δ and *sir2*Δ *hst1*Δ mutants, but not the *hst1*Δ mutant (Fig 4B, middle panel), indicating there was indeed a *sir2*Δ-induced pseudodiploid effect that suppressed CIN (Fig 4B, middle panel). Aging increased sectoring in each strain even when *HMR* was deleted, indicating the aging-associated CIN factor was unrelated to mating type control.

Even though SCC was unaffected by forced cohesin depletion, rDNA array condensation and stability were significantly impaired [37]. We therefore hypothesized that age-induced

chromosome instability could be related to rDNA instability caused by natural Sir2 and cohesin depletion. To address this idea, *FOB1* was deleted to stabilize the rDNA and the sectoring phenotype retested. As shown in Fig 4B (right panel), the age-associated increase in chromosome instability for each mutant was generally reduced to that observed with young *FOB1*$^{+}$ cells (Fig 4B, left panel), consistent with rDNA instability driving overall CIN.

What could be the mechanistic connection between the rDNA and centromeres? Previous Hi-C analysis of the yeast genome and fluorescence microscopy of nucleolar proteins positioned the rDNA off to one side of the nucleus, apparently secluded from the rest of the genome [44, 45]. The repetitive nature of rDNA precludes it from appearing in Hi-C contact maps, but closer inspection of chromosome XII at 10 kb resolution indicated a clear interaction between unique sequences flanking the centromere-proximal (left) edge of the array and *CEN12* (Fig 4C). Further analysis of observed/expected contacts using HOMER revealed a looped structure between the rDNA and *CEN12* (Fig 4D), which was recently reported to occur during anaphase [46]. Interestingly, all centromeres in the yeast genome, including *CEN12*, cluster together in Hi-C contact maps (Fig 4E; [44]), which by default also places them in contact with the left flank of the rDNA. Taken together, these results suggest that the rDNA comes in close contact with centromeres during mitosis, providing a potential window of time for rDNA instability to physically impact the integrity of general chromosome segregation.

Growth on galactose induces CIN and shortens RLS

Since Sir2 and cohesin are both naturally depleted from replicatively aging yeast cells, and mild Sir2 overexpression extends RLS [23], we hypothesized that manipulating cohesin expression levels would also impact CIN and RLS. We initially attempted to overexpress the

Mcd1 subunit from a galactose inducible *GAL1* promoter and then measure minichromosome loss frequency by counting ½ sectored colonies. However, simply growing the reporter strain in galactose-containing media, even with an empty expression cassette, resulted in severe minichromosome loss compared to glucose-containing media (Figs 5A and B). This effect was specific to galactose, as growth with another non-preferred carbon source (raffinose) had no effect on sectoring (Figs 5A and 5B). We next measured RLS with the minichromosome reporter strain on YEP plates with 2% glucose, galactose, or raffinose. As shown in Fig 5C, galactose decreased the mean RLS by ~50% compared to glucose (9.2 vs. 18.9 divisions), while raffinose only marginally decreased lifespan to an average of 15.5 cell divisions. To confirm the galactose effect on RLS was not specific to the minichromosome strain, RLS assays were repeated with the well-characterized strains BY4741 (*MAT*a) and BY4742 (*MAT*α). Again, a significant decrease in mean lifespan was observed for BY4741 (17.7 divisions) and BY4742 (18.9 divisions) on galactose as compared to glucose (24.3 and 24.2 divisions, respectively) (Fig 5D), suggesting that galactose triggers high rates of CIN through an unknown mechanism that also shortens RLS.

RLS is modulated by Mcd1 expression levels

To circumvent the use of galactose for *MCD1* overexpression we turned to an inducible "Tet-On" promoter that is activated by doxycycline [47]. Strains harboring this integrated cassette transcriptionally overexpressed *MCD1* approximately 7-fold compared to the empty vector control (S4 Fig). *MCD1* was overexpressed in a "WT" strain (JH5275b) and a mutant (JH5276b) containing an ochre stop codon in the *MCD1* open-reading frame (*mcd1L12STOP*) that reduced Mcd1 protein levels to ~30% of normal [37]. With an empty pRS405 control vector integrated, *mcd1L12STOP* exhibited a 40% reduction in mean RLS (9.9 divisions) compared to

287 WT (16.5 divisions), and overexpressing *MCD1* almost fully restored mean RLS to the mutant
288 (14.7 divisions) (Fig 6A). Especially intriguing was the observation that *MCD1* overexpression
289 extended mean RLS in the WT background to 19.6 division, an increase that was primarily due
290 to improved survival during the first ~15 divisions, followed by a steeper decline later (Fig 6A).
291 This biphasic pattern was highly reproducible, as it was observed in three independent RLS
292 experiments. Mechanistically, there could be a secondary age-related event at the RLS mid-point
293 that is beyond rescue by ectopic *MCD1* expression. Alternatively, doxycycline-induction could
294 eventually be attenuated due to the extended incubation times of RLS assays. Either way, the
295 results clearly indicate that similar to Sir2, the Mcd1 subunit of cohesin is a dosage-dependent
296 longevity factor.

297 Previous studies reported that Sir2 was required for efficient cohesin association with the
298 rDNA due to silencing of E-pro [16, 31], implying that Sir2 was upstream of cohesin. This
299 functional relationship could be more complex in the context of RLS, especially since both
300 factors are depleted with age. To explore further, we tested whether *SIR2* overexpression could
301 rescue the short RLS of an Mcd1-depleted *mcd1L12STOP* strain by integrating a second copy of
302 *SIR2* (2x*SIR2*) at the *LEU2* locus. As shown in Fig 6B, 2x*SIR2* partially rescued mean RLS of
303 the *mcd1L12STOP* strain (14.1 versus 9.9 divisions), and also increased maximum RLS of the
304 WT strain as expected. Reciprocally, we asked whether *MCD1* overexpression could suppress
305 the short RLS of a *sir2*Δ *hst1*Δ mutant. The double mutant was chosen to avoid any redundancy
306 between the two sirtuins. Mean RLS was clearly not increased by *MCD1* overexpression as
307 compared to empty vector (10.1 versus 9.7 divisions, Fig 6C), confirming that *SIR2* was
308 upstream of *MCD1* in regulating RLS.

Considering the strong depletion of cohesin from rDNA in old cells (Fig 2G), and extended RLS when *MCD1* was overexpressed (Fig 6A), we next tested whether aging-induced rDNA instability was suppressed by *MCD1* overexpression using a reporter strain harboring *ADE2* in the rDNA array [23]. There was a large increase of red/white sectoring (marker loss) in old cells that was suppressed upon *MCD1* overexpression (Fig 6D). In the absence of *SIR2*, however, red/white sectoring was high in both young and old cells when the empty vector (pRF10) was integrated, and *MCD1* overexpression did not significantly reduce rDNA instability in either population (Fig 6D), indicating that at least some Sir2 was required for Mcd1 to impact rDNA stability. We conclude that loss of Sir2 and cohesin in aging cells causes rDNA array instability that exacerbates CIN.

RLS extension by CR correlates with improved chromosome stability

Reducing glucose concentration in the growth medium is effective at extending RLS and is considered a form of caloric restriction (CR) for yeast [48, 49]. There have been several hypotheses put forth for the underlying mechanisms, including stabilization of the rDNA [21]. Since *MCD1* overexpression suppressed rDNA recombination and extended RLS, we hypothesized that CR would suppress the shortened RLS of a cohesion-depleted *mcd1L12STOP* mutant strain. Indeed, CR extended RLS of both the WT and *mcd1L12STOP* strains (Fig 7A). However, the suppression was apparently not due to maintenance of global cohesion levels because steady state Mcd1-13xMyc was still depleted in restricted old cells (Fig 7B). CR also strongly suppressed minichromosome loss in young and aged cells, even in the *sir2*Δ *hst1*Δ double mutant (Fig 7C). Importantly, this CR effect also correlated with almost complete rescue of RLS for the *sir2*Δ *hst1*Δ mutant (Fig 7D). Taken together, the results reveal a new mechanism

for RLS extension by CR, whereby stabilization of the rDNA locus helps maintain general mitotic chromosome stability to protect against aneuploidy.

Discussion

Nuclear protein depletion during replicative aging as a paradigm for aging pathologies

During this study the majority of chromatin-associated proteins analyzed by western blotting were depleted in replicatively aged yeast cells. The only protein unaffected by age, other than the vacuolar Vma2 control, was Sir3. A similar proportion of homologous recombination proteins were depleted in an independent analysis of old cells, with Rad52 the only one not affected [50]. These results indicate there is at least some selectivity to the depletion of nuclear proteins in old cells. However, the large number of depleted factors also makes it likely that targeted nuclear protein deficiency could lead to multiple age-associated phenotypes. Replicatively aging yeast cells appear especially susceptible to this phenomenon, as even total core histone levels are depleted [51]. Evidence also exists for histone depletion during aging of metazoan organisms, including mammals (reviewed in [52]). More generally, global protein turnover is elevated in cells from prematurely aging progeria patients, which may trigger higher translation rates [53]. This is significant because reducing translation is a means of extending lifespan in multiple organisms [54]. Ribosomal proteins appear to accumulate in old cells [55], again consistent with protein synthesis being a driver of aging [56]. The mechanism(s) driving nuclear protein depletion in old yeast mother cells remain unclear.

The specificity for Sir2/Sir4 depletion over Sir3 is intriguing given that Sir2 and Sir4 form a tight complex that allosterically stimulates the deacetylase activity of Sir2 [57]. Sir2/Sir4 also binds to H4K16-acetylated chromatin independent of Sir3, which is subsequently recruited

355 to complete the SIR holocomplex once H4K16 is deacetylated [36]. The mechanism for Sir2/Sir4
356 depletion from old cells remains uncharacterized, though in non-aging cell populations the
357 stability/turnover of Sir4, but not Sir2, is mediated by the E3 ubiquitin ligase San1 [58], which
358 has also been implicated as a quality control E3 ligase for mutated/unfolded nuclear proteins
359 [59]. Whether San1 controls Sir4 stability during aging remains unknown, but since Sir4 is more
360 severely depleted than Sir2 in old cells (Figs 2A and 2C), Sir4 could be selectively depleted from
361 the SIR complex, thus leaving Sir2 unprotected and then subject to turnover through a different
362 mechanism. Alternatively, Sir2/Sir4 could be equally depleted as a complex from telomeres and
363 the *HM* loci (not necessarily via San1), leaving the nucleolar pool of Sir2/RENT as more
364 resistant to aging. Under this scenario, protecting the integrity of the rDNA array could take
365 precedence over other heterochromatic domains. Interestingly, the *Schizosaccharomyces pombe*
366 San1 ortholog has also been implicated in a chaperone-assisted degradation pathway that
367 functions in quality control of kinetochores to promote chromosome stability [60].
368 Sir2 depletion in replicatively aged yeast cells is reminiscent of Sirt1 depletion in serially
369 passaged mouse embryonic fibroblasts (MEFs), which correlates with declining mitotic activity
370 [61]. Sir2 and Sirt1 are both known to function in regulating DNA replication origins [62, 63],
371 and the effect of deleting *SIR2* on early origin firing is thought to be mediated by competition for
372 limiting factors with the repeated rDNA origins [64]. Furthermore, CR has been proposed to
373 extend RLS by reducing rDNA origin firing, which improves overall genome replication [65].
374 Therefore, depleted cohesin in old cells could potentially cause rDNA instability by impacting
375 DNA replication.
376
377 **A precarious balance between rDNA and centromeric cohesion**

Sister chromatid cohesion (SCC) ensures chromosomes are not segregated until the Mcd1/Scc1 cohesin subunit is cleaved in response to a mitotic spindle checkpoint signal that all chromosomes are properly attached to microtubules and aligned at the metaphase plate (reviewed in [24]). Cohesin is also critical during meiosis, and it is well established in mammals that SCC defects occur in the oocytes of older mothers, causing meiotic chromosome missegregation events during both anaphase I and II [66]. This phenomenon is believed to be a major mechanism for increased aneuploidy risk that usually results in embryonic lethality, or in the case of chromosome 21 trisomy, Down's syndrome in children. The meiotic cohesin subunit Rec8 is depleted in the oocytes of older mice, as is Shugoshin (Sgo2), which normally protects/maintains centromeric cohesin [67]. More recent experiments in *Drosophila* suggest that oxidative stress in aged oocytes contributes to the SCC defects [68]. Our results in replicatively aging yeast cells reveal that aging-induced cohesin depletion and the resulting chromosome missegregation can extend to mitotic cells. Though cohesin depletion or defects have not been reported for mammalian somatic cells, the mitotic spindle checkpoint protein BubR1 is depleted in dynamic somatic tissues such as spleen [69]. Deficiency of this protein results in premature aging phenotypes [69], while overexpression extends lifespan [70]. This is similar to the effects we observe with Mcd1 depletion and overexpression on yeast RLS. Interestingly, BubR1 is also a deacetylation target of Sirt2, which appears to stabilize the protein and extend lifespan, thus linking mitotic spindle checkpoint regulation to NAD^+ metabolism [71]. It remains unclear if Sir2, Hst1, or other sirtuins regulate the yeast BubR1 ortholog, Mad3, or additional checkpoint and kinetochore proteins.

SCC is the canonical function for cohesin, though the complex also functions in establishing and regulating genome organization at the level of chromatin structure, gene

regulation, and double strand break (DSB) repair (reviewed in [72]). Among these various processes, SCC at centromeres appears the most critical because artificial depletion of Mcd1 to <30% of normal levels results in preferential cohesin binding to pericentromeric regions rather than cohesin associated regions (CARs) on chromosome arms [37]. SCC was also well maintained in these strains at the expense of normal chromosome condensation, DNA repair, and rDNA stability [37]. In aged yeast cells we observed relative enrichment of Mcd1-myc at centromeres as compared to loss at the rDNA (IGS1) locus (Fig 2G), suggesting an attempt by cells to maintain centromere cohesion at all costs, similar to what occurred in the artificially depleted system. Despite maintaining the cohesin complex at centromeres, SCC was still impaired in the older cells, especially when tension was maintained. In contrast, an independent study that analyzed significantly older mother cells (~20 generations) than in our study (~6 generations) observed reduced cohesin enrichment at centromeres [50]. Collectively, the results suggest that centromere-associated cohesin is preferentially retained during the initial stages of replicative aging, but then eventually breaks down below a critical threshold in the oldest cells.

Numerous nuclear proteins are depleted in old yeast cells, not just cohesin subunits, so we hypothesize that defects in other nuclear processes mediated by such factors also contribute to SCC defects and chromosome instability either directly or indirectly. The depleted cohesin loading complex (Scc2/4) is an obvious candidate due to its role in loading cohesin onto chromatin. Similarly, the depleted Lrs4/Csm1(cohibin complex) is proposed to act as a cohesin clamp onto rDNA chromatin [73], and also functions at centromeres to maintain mitotic integrity [74]. Sir2 and Hst1 are also obvious candidates given the earlier finding that H4K16 deacetylation at centromeres by Sir2 helps maintain chromosome stability [26]. Hst1 also binds centromeric DNA *in vitro* and *in vivo* [75], though the functional relevance of that association

424 remains uncharacterized. The suppression of age-associated mini-chromosome loss in the
425 absence of *FOB1* clearly points to rDNA instability as an unexpected source of general CIN.
426 Such a relationship is reinforced by the observed depletion of nucleolar proteins Net1 and Lrs4
427 in old cells (Figs 2E and S2D), both of which are required for normal rDNA/nucleolar integrity
428 and stable cohesin association with the rDNA [14, 73, 76].

429 How could destabilization of the rDNA locus result in general chromosome instability
430 and shortened RLS? As depicted in Fig 4, unique sequence flanking the rDNA on chromosome
431 XII contacts the centromere of each chromosome, including XII. Whether the actual rDNA genes
432 contact centromeres remains unclear due to the limitations of Hi-C analysis with repetitive DNA.
433 However, specific regions of the rDNA were previously shown to associate with various non-
434 rDNA chromosomal regions using an anchored 4C approach [77]. Loss of cohesin from the
435 rDNA could potentially disrupt long-range interactions with centromeres or non-centromeric
436 regions of cohesin association that influence chromosome integrity. One potential mechanism
437 could be significant disruption of overall chromosome condensation during mitosis, as the
438 cohesin appears to play the major role in chromosome condensation in budding yeast instead of
439 the condensin complex [46], which is different from metazoan organisms where condensin is the
440 primary condensation machinery.

441 Interestingly, another class of nuclear factors depleted in old yeast cells are several DNA
442 repair proteins [50]. Consequently, the lack of proper DNA repair while the rDNA becomes
443 destabilized correlates with fragmentation of chromosome XII and the other chromosomes, with
444 rDNA sequences actually being transferred into the other chromosomes. It was proposed that
445 accumulation of breaks and rearrangements ultimately causes cell death during replicative aging.
446 Such cells were significantly older (>25 divisions) compared to the cells in our study, which

447 averaged 5-6 divisions. Alternatively, it is possible that these presumably random
448 rearrangements disrupt normal SCC, leading to CIN.
449
450 **Aneuploidy as an aging mechanism**
451 All 16 *S. cerevisiae* chromosomes harbor essential genes, so if a single chromosome is
452 lost from a haploid yeast cell, then the affected mother or daughter cell should become inviable
453 and no longer divide. Given the elevated frequency of chromosome loss during replicative aging,
454 the chances of generating an inviable mother cell during a replicative aging assay increases after
455 each subsequent division. Therefore, at least a portion of the replicative lifespan in haploid yeast
456 cells is controlled by the ability to maintain all 16 chromosomes. Complete loss of a
457 chromosome would not be an immediate viability issue for diploid cells, however, as the chances
458 of losing both homologs in a single mitosis are exceedingly rare. On the other hand, haploid
459 strains that are disomic for individual chromosomes are often short lived, with longer
460 chromosomes typically having larger effects [28]. It was hypothesized that such strains suffer
461 from proteotoxic stress due to inappropriate protein expression levels. Therefore, a similar
462 mechanism could shorten RLS in a diploid strain that is trisomic for an individual chromosome,
463 though this has not yet been tested. Aneuploidy is also a hallmark of aging in the germline [78],
464 and somatic tissues of mammals [70, 79], making it a conserved feature of aging from yeast to
465 humans.
466 Another exciting feature of this study is the suppression of CIN by CR growth conditions
467 that extend RLS. This effect was independent of the reduced cohesin levels in aged cells, and
468 even improved RLS of the cohesin-depleted strains. Since SCC is normal in the cohesin-depleted
469 strain [37], we hypothesize that CR reinforces other processes that are defective due to reduced

cohesin or other depleted factors that promote rDNA stability. Indeed, CR is known to suppress rDNA instability in yeast cells [80, 81], and improve overall genome replication efficiency [65]. Hi-C analysis also suggests there could be direct effects of rDNA structure on centromere function, which will be the focus of future investigation.

Methods

Yeast strains, plasmids, and media

Yeast strains were primarily grown at 30°C in Yeast Peptone Dextrose (YPD) or Synthetic Complete (SC) medium for strains bearing plasmids [82]. *SIR2, HST1*, or *FOB1* open reading frames were disrupted with one-step PCR-mediated gene replacement using *kanMX4*, *natMX4*, or *hphMX4* drug resistance markers, respectively. The *HMR* deletion by replacement with *hphMX4* spans sacCer3 genome coordinates of chrIII 293170-294330. All C-terminally 13xMyc (EQKLISEEDL) tagged proteins were fused at the endogenous loci of haploid MEP strains UCC5181 and UCC5179, followed by crossing to generate homozygous diploids. All deletions and fusions were confirmed by colony PCR, western blotting, or both. pRF4 was constructed by PCR amplifying the *MCD1* open reading frame from ML1 genomic DNA and ligating into *Pst*I and *Not*I sites of pCM252, a tetracycline/doxycycline inducible overexpression vector available from Euroscarf (http://www.euroscarf.de). pRF10 and pRF11 were constructed by removing the expression cassette by *Pvu*II blunt end digestion of pCM252 and pRF4, respectively, and ligating it between the *Pvu*II sites of pRS405 bearing the *LEU2*, thus replacing the *TRP1* marker with *LEU2*. pSB760 and pSB766 are integrating and *2μ LEU2* vectors, respectively, bearing a single copy of *SIR2* [83]. All strains used in this work are listed in S1 Table and all primers are listed in S2 Table.

493

494 **Old yeast cell isolation**

495 Old yeast cell enrichment was based on MEP (Mother Enrichment Program) strains [33,
496 34]. For all assays, 1 µL of stationary phase culture was inoculated into 100 mL of YPD medium
497 and then grown into log phase. Approximately $1x10^8$ cells were harvested, and centrifuged cell
498 pellets washed 3 times with 1x phosphate buffered saline (PBS). Cells were then resuspended in
499 1 mL of PBS and mixed with 5 mg of Sulfo-NHS-LC-Biotin (Pierce) per $1x10^8$ cells for 30
500 minutes at room temperature. After biotin labeling, $5x10^7$ cells were added to 1.5 L YPD cultures
501 containing 1µM estradiol, and 100 µg/mL ampicillin to prevent bacterial contamination. These
502 cultures were allowed to grow for 24 hours before being processed in a downstream assay
503 specific manner (see below). For non-MEP strain backgrounds, estradiol was not added to the
504 cultures.

505

506 **Old cell western blots**

507 Two large scale cultures (1.5 L) were used for each western blot experiment
508 corresponding to approximately $2x10^7$ total old cells after purification. Cells were pelleted using
509 a Sorvall RC-5B Plus centrifuge with an SLA-3000 rotor at 2000 rpm, and then resuspended at a
510 density of $6x10^8$ cells/mL in RNAlater (Ambion) for 45 minutes in two separate conical tubes.
511 Following fixation, cells were pelleted and resuspended in 45 mL of cold 1xPBS, 2 mM EDTA
512 in 50 mL conical tubes. The mixture was incubated at 4°C for 30 min with 800 µL of
513 Streptavidin MicroBeads (Miltenyi Biotec), which were then purified through an autoMACS Pro
514 Cell Separator using the posseld2 program (UVA flow cytometry core facility). A 20 µL aliquot
515 of each output was used for bud scar counting using calcofluor white staining, before combining

the isolated samples into a single microfuge tube. Samples were frozen at -80°C before protein extraction. Thawed cells were vortexed twice for 1 min in 20% TCA (trichloroacetic acid) with ~100 µL of acid washed glass beads with a brief cooling period in between vortexing. Beads were allowed to settle before removing the supernatant to a fresh microfuge tube. A 250 µL wash of 5% TCA was applied twice to the beads and pooled with the initial lysis sample. Proteins were precipitated at 10,000 rpm in a microfuge for 5 min at 4°C. The pellets were resuspended in 50 µL of 1x SDS sample buffer (50 mM Tris-HCl pH 6.8, 2% SDS, 10% Glycerol, 3.6 M 2-mercaptoethanol) and neutralized with 30 µL of 1M Tris-HCl, pH 8.0. Samples were run on a 9% (w/v) SDS-polyacrylamide gel and transferred to an Immobilon-P membrane (Millipore). Membranes were incubated for 1 hour at room temperature in 1xTBST + 5% non-fat milk with primary antibodies (1:2000 α-Myc 9E10, 1:5000; α-Vma2 (Life Technologies); 1:5000 α-Sir2 (Santa Cruz Biotechnology); 1:1000 α-Sir4 (Santa Cruz Biotechnology); 1:1000 α-Sir3 (Santa Cruz Biotechnology). HRP-conjugated secondary antibodies (Promega) were diluted 1:5000, and detected using chemiluminescence with HyGLO (Denville Scientific).

ChIP Assays with old and young cells populations

Two 1.5 L cultures were used for each biological replicate sample. After centrifugation, cells were washed with 1xPBS and resuspended in 45 mL of 1xPBS and incubated with 800 µL of streptavidin microbeads, followed by sorting with the autoMACS Pro Cell Separator. Sorted cells were immediately crosslinked with 1% formaldehyde for 20 min at room temperature, then transferred to screw cap microcentrifuge tubes and the pellets flash frozen in liquid nitrogen. Cells were thawed and lysed in 600 µL FA140 Lysis buffer (50 mM HEPES, 140 mM NaCl, 1% Triton X-100, 1 mM EDTA, 0.1% SDS, 0.1 mM PMSF, 1x protease inhibitor cocktail; Sigma)

by shaking with acid-washed glass beads in a Mini-Bead beater (Biospec Products). Cell lysates were recovered and sonicated for 30 cycles of 30 sec "on" and 30 sec "off" in a Diagenode Bioruptor followed by centrifugation at 16,000 x g. A 1/10th supernatant volume input was taken for each sample and crosslinking reversed by incubating overnight at 65°C in 150 µL elution buffer (TE, 1% SDS). The remaining supernatant was used for immunoprecipitation overnight at 4°C with 5 µg of primary antibody and 30 µL of protein G magnetic beads (Pierce), followed by washing 1x with FA-140 buffer, 2x with FA-500 buffer (FA-140 with 500 mM NaCl), and 2x with LiCl solution (10 mM Tris-HCl, pH 8.0, 250 mM LiCl, 0.5% NP-40, 0.5% SDS, 1 mM EDTA). DNA was eluted twice with 75 µL of elution buffer in a 65°C water bath for 15 min. The eluates were combined and crosslinking reversed. Input and ChIP DNA samples were purified by an Invitrogen PureLink™ PCR purification kit. Finally, ChIP DNA was quantified by real-time PCR and normalized to the input DNA signal. Young cells were collected from flow through out of the autoMACS cell sorter and then processed as described for the aged cells. For ChIP assays on unsorted populations, cells were grown to log phase in 100 mL YPD before formaldehyde cross-linking for 20 min at 30°C while shaking. Additionally, 2.5 mg of protein was used for the IP instead of the entire lysate, and the chromatin solution was sonicated for 50 cycles rather than 30.

ChIP-Seq Library Preparation

Chromatin was prepared in a similar manner to old cell ChIP assays with the following exceptions. Cells were grown to log phase in 200 mL YPD and fixed for 20 min with 1% formaldehyde. Lysate volumes were adjusted to 4 mL in FA-140 lysis buffer and sonicated 5 times with a Branson 250 Digital Sonifier for 30 sec at 70% amplitude. Samples were cooled on

ice for at least 1 min between sonication periods. The lysate was split into 3 microcentrifuge tubes and spun for 10 min at 10,000 rpm in a microfuge at 4°C. The entire supernatant from 1 tube was used for immunoprecipitation overnight with 15 µg of α-Myc 9E10 antibody and 30 µL of protein G magnetic beads (Pierce). After washing, elution, and reverse cross-linking, 100 mg of Proteinase K was added for 2 hr at 42°C. Chromatin was purified in a Zymogen DNA Clean and Concentrator-5 Kit and quantified using a Qubit fluorometric device. A minimum of 20 ng of DNA was used as input for NEBNext® library construction. ML150 libraries were sequenced on an Illumina Nextseq and ML163 libraries on an Illumina Miseq by the UVA Genome Analysis and Technology Core. Sequencing files are available at GEO accession number GSE117037. Sequencing reads were mapped to the sacCer3 genome using bowtie2 with default settings. Corresponding bam files were further processed to produce the coverage plots shown in Fig 1 with the Deeptools package of Galaxy (https://usegalaxy.org/).

Sister chromatid cohesion assay

From 50 mL log phase SC cultures of strains 3349-1B, 3312-7A, and 3460-2A, $5x10^7$ cells were washed and biotinylated as described in the Old Cell Isolation section. This population was transferred into a 1.5 L SC culture and allowed to grow for 12 hr. The original biotinylated population was then purified by incubation with 300 µL of streptavidin micro beads followed by gravity filtration through a Miltenyi LS column. The column was washed twice with 5 ml of PBS and the enriched cell/bead population was aged for an additional 12 hr in a fresh 1.5 L SC culture before being purified for a second time with an additional 200 µL of beads. Eluted cells (still bound to beads) were processed as described below for young cells.

584 From the original log phase culture, $5x10^7$ cells were arrested in a fresh 50 mL SC culture
585 containing 10 µg/mL nocodazole for 1.5 hr. For the *mcd1-1* strain 3312-7A, cells were also
586 shifted to 36°C at this time. Bud scars were stained with the addition of 1 mL of supernatant
587 from a solution of PBS and 5 mg of Calcofluor white that was centrifuged to eliminate
588 aggregates. Non-arrested cells were directly stained with calcofluor. Cells were then pelleted and
589 washed in PBS. Following staining, 200 µL of 4% paraformaldehyde was added directly to the
590 cell pellet and allowed to crosslink for 15 min at room temperature. The cell pellet was washed
591 once with PBS and resuspended in ~100-200 µL of 0.1 $MKPO_4$/1 M sorbitol, pH 6.5. Images
592 were captured with a Zeiss Axio Observer z1 widefield microscope using a 64x oil objective
593 lens.
594
595 **Replicative lifespan assays**
596 Lifespan assays were carried out essentially the same as previously described [84].
597 Briefly, small aliquots of log phase cultures were dripped in a straight line onto solid agar YPD
598 with 2% glucose. From the initial populations, a minimum of 32 virgin daughter cells were
599 picked for lifespan assays with daughter cells being selectively pulled away from mother cells
600 using a fiberoptic dissection needle and on a Nikon Eclipse 400 microscope. All virgin daughters
601 were required to bud at least one time to be included in the experiment and dissection was
602 carried out over the course of several days with temporary incubation at 4°C in between
603 dissection periods to stop division. Cells were considered dead when they stopped dividing for a
604 minimum of 2 generation times (180 min).
605
606 **Chromosome loss (sectoring) assay**

607 The colony sectoring assay was performed on SC plates with adenine limited to 80 µM.
608 Frequency of mini-chromosome loss represents the number of ½ or ¼ red/white sectored
609 colonies divided by the sum of sectored and white colonies. Cells were plated to an approximate
610 density of 500 cells/plate based on counts from a Brightline hemacytometer. Any plates bearing
611 greater than 1000 cells were discarded. Three biological replicates of each strain were
612 performed, with at least 10 plates counted per replicate. For old cell populations, ~5x10^6
613 biotinylated cells were aged in 1.5 L of YPD for 24 hr. Cells were incubated with 300 µL of
614 streptavidin magnetic beads (New England Biolabs) and manually washed 4 times with PBS on a
615 magnetic stand, then plated onto the limiting adenine SC plates such that ~500 colonies
616 appeared. Bud scars were not counted because the size of the beads prohibited visualization.
617
618 **RT-qPCR measurement of *MCD1* overexpression**
619 Doxycycline was added to log phase cultures at a concentration of 2 µg/mL for 6 hr in
620 order to induce expression of MCD1 from pRF4. Total RNA was extracted using a standard acid
621 phenol extraction protocol [85]. cDNA was created from ~1 µg of RNA using a Verso cDNA
622 synthesis kit (Thermo Fisher). *MCD1* expression levels were quantified on an Applied
623 Biosystems StepOne real time PCR machine with primers JS2844 and JS2949, and normalized to
624 actin transcript levels (primers JS1146 and JS1147).
625
626 **Hi-C analysis**
627 Log-phase cultures were cross-linked with 3% formaldehyde for 20 min and quenched
628 with a 2x volume of 2.5M Glycine. Cell pellets were washed with dH_2O and stored at -80°C.
629 Thawed cells were resuspended in 5 ml of 1X NEB2 restriction enzyme buffer (New England

Biolabs) and poured into a pre-chilled mortar containing liquid N_2. Nitrogen grinding was performed twice as previously described [86], and the lysates were then diluted to an OD_{600} of 12 in 1x NEB2 buffer. 500 µl of cell lysate was used for each Hi-C library as follows. Lysates were solubilized by the addition of 50 µl 1% SDS and incubation at 65°C for 10 min. 55 µl of 10% TritonX-100 was added to quench the SDS, followed by 10 µl of 10X NEB2 buffer and 15 µl of *Hin*dIII (New England Biolabs, 20 U/µl) to digest at 37°C for 2 hr. An additional 10 µl of *Hin*dIII was added for digestion overnight. The remainder of the protocol was based on previously published work with minor exceptions [87], see supplemental experimental procedures for details. Hi-C sequencing libraries were prepared with reagents from an Illumina Nextera Mate Pair Kit (FC-132-1001) using the standard Illumina protocol of End Repair, A-tailing, Adapter Ligation, and 12 cycles of PCR. PCR products were size selected and purified with AMPure XP beads before sequencing with an Illumina Miseq or Hiseq.

Author Contributions

Conceptualization; R.D.F. and J.S.S.; Methodology, R.D.F., M.L. and J.S.S.; Software, R.D.F.; Strain Creation and Validation, R.D.F., N.M., E.F., and M.L.; Plasmid Creation and Validation, R.D.F., E.F., and M.L; Formal Analysis, R.D.F.; Data Curation, R.D.F.; Writing-Original Draft, R.D.F. and J.S.S.; Writing Review & Editing, R.D.F., M.L., and J.S.S; Supervision, J.S.S.; Project Administration, J.S.S.; Funding Acquisition, J.S.S.

Acknowledgments

We thank Dan Gottschling and all lab members for kindly providing yeast strains and initial advice on using the MEP system. Stefan Bekiranov, Job Dekker, Jon Belton, Maitreya Dunham,

Ivan Liachko, Maxim Imakev, and Anton Goloborodko all provided valuable advice on Hi-C protocols and analysis methods. We thank Doug Koshland for providing the Mcd1 reduction and cohesion assay strains, and Matt Kaeberlein for rDNA marker loss strains. Special thanks to Todd Stukenberg for microscopy assistance. Lastly, thanks to David Auble for critically reading the manuscript and providing comments prior to submission. We declare no conflicts of interest.

References

1. Mortimer RK, Johnston JR. Life span of individual yeast cells. Nature. 1959;183(4677):1751-2. PMID: 13666896.

2. Wasko BM, Kaeberlein M. Yeast replicative aging: a paradigm for defining conserved longevity interventions. FEMS Yeast Res. 2014;14(1):148-59. PMID: 24119093.

3. Buck SW, Gallo CM, Smith JS. Diversity in the Sir2 family of protein deacetylases. J Leukoc Biol. 2004;75(6):939-50. PMID: 14742637.

4. Gomes AP, Price NL, Ling AJ, Moslehi JJ, Montgomery MK, Rajman L, et al. Declining NAD^+ induces a pseudohypoxic state disrupting nuclear-mitochondrial communication during aging. Cell. 2013;155(7):1624-38. PMID: 24360282.

5. Brachmann CB, Sherman JM, Devine SE, Cameron EE, Pillus L, Boeke JD. The *SIR2* gene family, conserved from bacteria to humans, functions in silencing, cell cycle progression, and chromosome stability. Genes Dev. 1995;9(23):2888-902. PMID: 7498786.

6. Rine J, Herskowitz I. Four genes responsible for a position effect on expression from *HML* and *HMR* in *Saccharomyces cerevisiae*. Genetics. 1987;116(1):9-22. PMID: 3297920.

7. Gartenberg MR, Smith JS. The nuts and bolts of transcriptionally silent chromatin in *Saccharomyces cerevisiae*. Genetics. 2016;203(4):1563-99. PMID: 27516616.

676 8. Dang W, Steffen KK, Perry R, Dorsey JA, Johnson FB, Shilatifard A, et al. Histone H4
677 lysine 16 acetylation regulates cellular lifespan. Nature. 2009;459(7248):802-7. PMID:
678 19516333.
679 9. Smeal T, Claus J, Kennedy B, Cole F, Guarente L. Loss of transcriptional silencing
680 causes sterility in old mother cells of *S. cerevisiae*. Cell. 1996;84(4):633-42. PMID: 8598049.
681 10. Schlissel G, Krzyzanowski MK, Caudron F, Barral Y, Rine J. Aggregation of the Whi3
682 protein, not loss of heterochromatin, causes sterility in old yeast cells. Science.
683 2017;355(6330):1184-7. PMID: 28302853.
684 11. Bryk M, Banerjee M, Murphy M, Knudsen KE, Garfinkel DJ, Curcio MJ. Transcriptional
685 silencing of Ty1 elements in the *RDN1* locus of yeast. Genes Dev. 1997;11(2):255-69. PMID:
686 9009207.
687 12. Smith JS, Boeke JD. An unusual form of transcriptional silencing in yeast ribosomal
688 DNA. Genes Dev. 1997;11(2):241-54. PMID: 9009206.
689 13. Shou W, Seol JH, Shevchenko A, Baskerville C, Moazed D, Chen ZW, et al. Exit from
690 mitosis is triggered by Tem1-dependent release of the protein phosphatase Cdc14 from nucleolar
691 RENT complex. Cell. 1999;97(2):233-44. PMID: 10219244.
692 14. Straight AF, Shou W, Dowd GJ, Turck CW, Deshaies RJ, Johnson AD, et al. Net1, a
693 Sir2-associated nucleolar protein required for rDNA silencing and nucleolar integrity. Cell.
694 1999;97(2):245-56. PMID: 10219245.
695 15. Li C, Mueller JE, Bryk M. Sir2 represses endogenous polymerase II transcription units in
696 the ribosomal DNA nontranscribed spacer. Mol Biol Cell. 2006;17(9):3848-59. PMID:
697 16807355.

16. Kobayashi T, Ganley AR. Recombination regulation by transcription-induced cohesin dissociation in rDNA repeats. Science. 2005;309(5740):1581-4. PMID: 16141077.

17. Sinclair DA, Guarente L. Extrachromosomal rDNA circles--a cause of aging in yeast. Cell. 1997;91(7):1033-42. PMID: 9428525.

18. Defossez PA, Prusty R, Kaeberlein M, Lin SJ, Ferrigno P, Silver PA, et al. Elimination of replication block protein Fob1 extends the life span of yeast mother cells. Mol Cell. 1999;3(4):447-55. PMID: 10230397.

19. Kobayashi T, Horiuchi T. A yeast gene product, Fob1 protein, required for both replication fork blocking and recombinational hotspot activities. Genes Cells. 1996;1(5):465-74. PMID: 9078378.

20. Takeuchi Y, Horiuchi T, Kobayashi T. Transcription-dependent recombination and the role of fork collision in yeast rDNA. Genes Dev. 2003;17(12):1497-506. PMID: 12783853.

21. Ganley AR, Kobayashi T. Ribosomal DNA and cellular senescence: new evidence supporting the connection between rDNA and aging. FEMS Yeast Res. 2014;14(1):49-59. PMID: 24373458.

22. Ganley AR, Ide S, Saka K, Kobayashi T. The effect of replication initiation on gene amplification in the rDNA and its relationship to aging. Mol Cell. 2009;35(5):683-93. PMID: 19748361.

23. Kaeberlein M, McVey M, Guarente L. The SIR2/3/4 complex and SIR2 alone promote longevity in *Saccharomyces cerevisiae* by two different mechanisms. Genes Dev. 1999;13(19):2570-80. PMID: 10521401.

24. Marston AL. Chromosome segregation in budding yeast: sister chromatid cohesion and related mechanisms. Genetics. 2014;196(1):31-63. PMID: 24395824.

721 25. Wood AJ, Severson AF, Meyer BJ. Condensin and cohesin complexity: the expanding
722 repertoire of functions. Nat Rev Genet. 2010;11(6):391-404. PMID: 20442714.
723 26. Choy JS, Acuna R, Au WC, Basrai MA. A role for histone H4K16 hypoacetylation in
724 *Saccharomyces cerevisiae* kinetochore function. Genetics. 2011;189(1):11-21. PMID: 21652526.
725 27. Holmes SG, Rose AB, Steuerle K, Saez E, Sayegh S, Lee YM, et al. Hyperactivation of
726 the silencing proteins, Sir2p and Sir3p, causes chromosome loss. Genetics. 1997;145(3):605-14.
727 PMID: 9055071.
728 28. Sunshine AB, Ong GT, Nickerson DP, Carr D, Murakami CJ, Wasko BM, et al.
729 Aneuploidy shortens replicative lifespan in *Saccharomyces cerevisiae*. Aging Cell.
730 2016;15(2):317-24. PMID: 26762766.
731 29. Glynn EF, Megee PC, Yu HG, Mistrot C, Unal E, Koshland DE, et al. Genome-wide
732 mapping of the cohesin complex in the yeast *Saccharomyces cerevisiae*. PLoS Biol.
733 2004;2(9):E259. PMID: 15309048.
734 30. Li M, Valsakumar V, Poorey K, Bekiranov S, Smith JS. Genome-wide analysis of
735 functional sirtuin chromatin targets in yeast. Genome Biol. 2013;14(5):R48. PMID: 23710766.
736 31. Kobayashi T, Horiuchi T, Tongaonkar P, Vu L, Nomura M. SIR2 regulates
737 recombination between different rDNA repeats, but not recombination within individual rRNA
738 genes in yeast. Cell. 2004;117(4):441-53. PMID: 15137938.
739 32. Stephens AD, Quammen CW, Chang B, Haase J, Taylor RM, 2nd, Bloom K. The spatial
740 segregation of pericentric cohesin and condensin in the mitotic spindle. Mol Biol Cell.
741 2013;24(24):3909-19. PMID: 24152737.

742 33. Lindstrom DL, Gottschling DE. The mother enrichment program: a genetic system for
743 facile replicative life span analysis in *Saccharomyces cerevisiae*. Genetics. 2009;183(2):413-22.
744 PMID: 19652178.
745 34. Lindstrom DL, Leverich CK, Henderson KA, Gottschling DE. Replicative age induces
746 mitotic recombination in the ribosomal RNA gene cluster of *Saccharomyces cerevisiae*. PLoS
747 Genet. 2011;7(3):e1002015. PMID: 21436897.
748 35. Moazed D, Kistler A, Axelrod A, Rine J, Johnson AD. Silent information regulator
749 protein complexes in Saccharomyces cerevisiae: a SIR2/SIR4 complex and evidence for a
750 regulatory domain in SIR4 that inhibits its interaction with SIR3. Proc Natl Acad Sci USA.
751 1997;94(6):2186-91. PMID: 9122169.
752 36. Oppikofer M, Kueng S, Martino F, Soeroes S, Hancock SM, Chin JW, et al. A dual role
753 of H4K16 acetylation in the establishment of yeast silent chromatin. EMBO J.
754 2011;30(13):2610-21. PMID: 21666601.
755 37. Heidinger-Pauli JM, Mert O, Davenport C, Guacci V, Koshland D. Systematic reduction
756 of cohesin differentially affects chromosome segregation, condensation, and DNA repair. Curr
757 Biol. 2010;20(10):957-63. PMID: 20451387.
758 38. Guacci V, Koshland D. Cohesin-independent segregation of sister chromatids in budding
759 yeast. Mol Biol Cell. 2012;23(4):729-39. PMID: 22190734.
760 39. Unal E, Heidinger-Pauli JM, Kim W, Guacci V, Onn I, Gygi SP, et al. A molecular
761 determinant for the establishment of sister chromatid cohesion. Science. 2008;321(5888):566-9.
762 PMID: 18653894.

763 40. Guacci V, Koshland D, Strunnikov A. A direct link between sister chromatid cohesion
764 and chromosome condensation revealed through the analysis of *MCD1* in *S. cerevisiae*. Cell.
765 1997;91(1):47-57. PMID: 9335334.
766 41. Spencer F, Gerring SL, Connelly C, Hieter P. Mitotic chromosome transmission fidelity
767 mutants in *Saccharomyces cerevisiae*. Genetics. 1990;124(2):237-49. PMID: 2407610.
768 42. Hickman MA, Rusche LN. Substitution as a mechanism for genetic robustness: the
769 duplicated deacetylases Hst1p and Sir2p in *Saccharomyces cerevisiae*. PLoS Genet.
770 2007;3(8):e126. PMID: 17676954.
771 43. Li M, Petteys BJ, McClure JM, Valsakumar V, Bekiranov S, Frank EL, et al. Thiamine
772 biosynthesis in *Saccharomyces cerevisiae* is regulated by the NAD^+-dependent histone
773 deacetylase Hst1. Mol Cell Biol. 2010;30(13):3329-41. PMID: 20439498.
774 44. Duan Z, Andronescu M, Schutz K, McIlwain S, Kim YJ, Lee C, et al. A three-
775 dimensional model of the yeast genome. Nature. 2010;465(7296):363-7. PMID: 20436457.
776 45. Gotta M, Strahl-Bolsinger S, Renauld H, Laroche T, Kennedy BK, Grunstein M, et al.
777 Localization of Sir2p: the nucleolus as a compartment for silent information regulators. EMBO J.
778 1997;16(11):3243-55. PMID: 9214640.
779 46. Schalbetter SA, Goloborodko A, Fudenberg G, Belton JM, Miles C, Yu M, et al. SMC
780 complexes differentially compact mitotic chromosomes according to genomic context. Nat Cell
781 Biol. 2017;19(9):1071-80. PMID: 28825700.
782 47. Belli G, Gari E, Piedrafita L, Aldea M, Herrero E. An activator/repressor dual system
783 allows tight tetracycline-regulated gene expression in budding yeast. Nucleic Acids Res.
784 1998;26(4):942-7. PMID: 9461451.

785 48. Jiang JC, Jaruga E, Repnevskaya MV, Jazwinski SM. An intervention resembling caloric
786 restriction prolongs life span and retards aging in yeast. FASEB J. 2000;14(14):2135-7. PMID:
787 11024000.
788 49. Lin SJ, Kaeberlein M, Andalis AA, Sturtz LA, Defossez PA, Culotta VC, et al. Calorie
789 restriction extends *Saccharomyces cerevisiae* lifespan by increasing respiration. Nature.
790 2002;418(6895):344-8. PMID: 12124627.
791 50. Pal S, Postnikoff SD, Chavez M, Tyler JK. Impaired cohesion and homologous
792 recombination during replicative aging in budding yeast. Sci Adv. 2018;4(2):eaaq0236. PMID:
793 29441364.
794 51. Hu Z, Chen K, Xia Z, Chavez M, Pal S, Seol JH, et al. Nucleosome loss leads to global
795 transcriptional up-regulation and genomic instability during yeast aging. Genes Dev.
796 2014;28(4):396-408. PMID: 24532716.
797 52. Song S, Johnson FB. Epigenetic mechanisms impacting aging: A focus on histone levels
798 and telomeres. Genes. 2018;9(4). PMID: 29642537.
799 53. Buchwalter A, Hetzer MW. Nucleolar expansion and elevated protein translation in
800 premature aging. Nat Commun. 2017;8(1):328. PMID: 28855503.
801 54. Mehta R, Chandler-Brown D, Ramos FJ, Shamieh LS, Kaeberlein M. Regulation of
802 mRNA translation as a conserved mechanism of longevity control. Adv Exp Med Biol.
803 2010;694:14-29. PMID: 20886753.
804 55. Janssens GE, Veenhoff LM. The natural variation in lifespans of single yeast cells is
805 related to variation in cell size, ribosomal protein, and division time. PLoS One.
806 2016;11(12):e0167394. PMID: 27907085.

807 56. Janssens GE, Meinema AC, Gonzalez J, Wolters JC, Schmidt A, Guryev V, et al. Protein
808 biogenesis machinery is a driver of replicative aging in yeast. eLife. 2015;4:e08527. PMID:
809 26422514.
810 57. Hsu HC, Wang CL, Wang M, Yang N, Chen Z, Sternglanz R, et al. Structural basis for
811 allosteric stimulation of Sir2 activity by Sir4 binding. Genes Dev. 2013;27(1):64-73. PMID:
812 23307867.
813 58. Dasgupta A, Ramsey KL, Smith JS, Auble DT. Sir Antagonist 1 (San1) is a ubiquitin
814 ligase. J Biol Chem. 2004;279(26):26830-8. PMID: 15078868.
815 59. Gardner RG, Nelson ZW, Gottschling DE. Degradation-mediated protein quality control
816 in the nucleus. Cell. 2005;120(6):803-15. PMID: 15797381.
817 60. Kriegenburg F, Jakopec V, Poulsen EG, Nielsen SV, Roguev A, Krogan N, et al. A
818 chaperone-assisted degradation pathway targets kinetochore proteins to ensure genome stability.
819 PLoS Genet. 2014;10(1):e1004140. PMID: 24497846.
820 61. Sasaki T, Maier B, Bartke A, Scrable H. Progressive loss of SIRT1 with cell cycle
821 withdrawal. Aging Cell. 2006;5(5):413-22. PMID: 16939484.
822 62. Hoggard TA, Chang F, Perry KR, Subramanian S, Kenworthy J, Chueng J, et al. Yeast
823 heterochromatin regulators Sir2 and Sir3 act directly at euchromatic DNA replication origins.
824 PLoS Genet. 2018;14(5):e1007418. PMID: 29795547.
825 63. Utani K, Aladjem MI. Extra View: Sirt1 acts as A gatekeeper of replication initiation to
826 preserve genomic stability. Nucleus. 2018;9(1):261-7. PMID: 29578371.
827 64. Yoshida K, Bacal J, Desmarais D, Padioleau I, Tsaponina O, Chabes A, et al. The histone
828 deacetylases sir2 and rpd3 act on ribosomal DNA to control the replication program in budding
829 yeast. Mol Cell. 2014;54(4):691-7. PMID: 24856221.

830 65. Kwan EX, Foss EJ, Tsuchiyama S, Alvino GM, Kruglyak L, Kaeberlein M, et al. A
831 natural polymorphism in rDNA replication origins links origin activation with calorie restriction
832 and lifespan. PLoS Genet. 2013;9(3):e1003329. PMID: 23505383.
833 66. Jessberger R. Age-related aneuploidy through cohesion exhaustion. EMBO Rep.
834 2012;13(6):539-46. PMID: 22565322.
835 67. Lister LM, Kouznetsova A, Hyslop LA, Kalleas D, Pace SL, Barel JC, et al. Age-related
836 meiotic segregation errors in mammalian oocytes are preceded by depletion of cohesin and Sgo2.
837 Curr Biol. 2010;20(17):1511-21. PMID: 20817533.
838 68. Perkins AT, Das TM, Panzera LC, Bickel SE. Oxidative stress in oocytes during
839 midprophase induces premature loss of cohesion and chromosome segregation errors. Proc Natl
840 Acad Sci USA. 2016;113(44):E6823-e30. PMID: 27791141.
841 69. Baker DJ, Jeganathan KB, Cameron JD, Thompson M, Juneja S, Kopecka A, et al.
842 BubR1 insufficiency causes early onset of aging-associated phenotypes and infertility in mice.
843 Nat Genet. 2004;36(7):744-9. PMID: 15208629.
844 70. Baker DJ, Dawlaty MM, Wijshake T, Jeganathan KB, Malureanu L, van Ree JH, et al.
845 Increased expression of BubR1 protects against aneuploidy and cancer and extends healthy
846 lifespan. Nat Cell Biol. 2013;15(1):96-102. PMID: 23242215.
847 71. North BJ, Rosenberg MA, Jeganathan KB, Hafner AV, Michan S, Dai J, et al. SIRT2
848 induces the checkpoint kinase BubR1 to increase lifespan. EMBO J. 2014;33(13):1438-53.
849 PMID: 24825348.
850 72. Uhlmann F. SMC complexes: from DNA to chromosomes. Nat Rev Mol Cell Biol.
851 2016;17(7):399-412. PMID: 27075410.

852 73. Huang J, Brito IL, Villen J, Gygi SP, Amon A, Moazed D. Inhibition of homologous
853 recombination by a cohesin-associated clamp complex recruited to the rDNA recombination
854 enhancer. Genes Dev. 2006;20(20):2887-901. PMID: 17043313.
855 74. Bitto A, Wang AM, Bennett CF, Kaeberlein M. Biochemical genetic pathways that
856 modulate aging in multiple species. Cold Spring Harb Perspect Med. 2015;5(11). PMID:
857 26525455.
858 75. Ohkuni K, Kitagawa K. Endogenous transcription at the centromere facilitates
859 centromere activity in budding yeast. Curr Biol. 2011;21(20):1695-703. PMID: 22000103.
860 76. Smith JS, Caputo E, Boeke JD. A genetic screen for ribosomal DNA silencing defects
861 identifies multiple DNA replication and chromatin-modulating factors. Mol Cell Biol.
862 1999;19(4):3184-97. PMID: 10082585.
863 77. O'Sullivan JM, Sontam DM, Grierson R, Jones B. Repeated elements coordinate the
864 spatial organization of the yeast genome. Yeast. 2009;26(2):125-38. MID: 19235779.
865 78. Nagaoka SI, Hassold TJ, Hunt PA. Human aneuploidy: mechanisms and new insights
866 into an age-old problem. Nat Rev Genet. 2012;13(7):493-504. PMID: 22705668.
867 79. Lushnikova T, Bouska A, Odvody J, Dupont WD, Eischen CM. Aging mice have
868 increased chromosome instability that is exacerbated by elevated Mdm2 expression. Oncogene.
869 2011;30(46):4622-31. PMID: 21602883.
870 80. Riesen M, Morgan A. Calorie restriction reduces rDNA recombination independently of
871 rDNA silencing. Aging Cell. 2009;8(6):624-32. PMID: 19732046.
872 81. Smith DL, Jr., Li C, Matecic M, Maqani N, Bryk M, Smith JS. Calorie restriction effects
873 on silencing and recombination at the yeast rDNA. Aging Cell. 2009;8(6):633-42. PMID:
874 19732044.

875 82. Matecic M, Smith DL, Pan X, Maqani N, Bekiranov S, Boeke JD, et al. A microarray-
876 based genetic screen for yeast chronological aging factors. PLoS Genet. 2010;6(4):e1000921.
877 PMID: 20421943.
878 83. Buck SW, Sandmeier JJ, Smith JS. RNA polymerase I propagates unidirectional
879 spreading of rDNA silent chromatin. Cell. 2002;111(7):1003-14. PMID: 12507427.
880 84. Steffen KK, Kennedy BK, Kaeberlein M. Measuring replicative life span in the budding
881 yeast. J Vis Exp. 2009;(28). PMID: 19556967.
882 85. Ausubel FM, Brent R, Kingston RE, Moore DD, Seidman JG, Smith JA, et al., editors.
883 Current Protocols in Molecular Biology. New York: John Wiley & Sons, Inc.; 2000.
884 86. Belton JM, Dekker J. Measuring Chromatin Structure in Budding Yeast. Cold Spring
885 Harb Protoc. 2015;2015(7):614-8. PMID: 26134912.
886 87. Burton JN, Liachko I, Dunham MJ, Shendure J. Species-level deconvolution of
887 metagenome assemblies with Hi-C-based contact probability maps. G3. 2014;4(7):1339-46.
888 PMID: 24855317.
889

890 ## Figure captions

891 **Fig 1. Cohesin distribution at the rDNA and centromeres in WT and *sir2*Δ cells. (A)**
892 Composite plot of Mcd1-13xMyc ChIP-Seq binding across the rDNA array from WT and *sir2*Δ
893 log-phase cells binned at 50bp resolution. **(B)** ChIP-qPCR quantifying Mcd1 enrichment at the
894 rDNA IGS1 region from log-phase cells. **(C)** Composite plot of Mcd1-13xMyc enrichment at all
895 16 yeast point centromeres. **(D)** ChIP-qPCR quantifying Mcd1 binding at two centromeres and a
896 pericentromeric site 15kb away from *CEN4*. (* $p<0.005$, two-tailed student t-test).

Fig 2. Depletion of Sir2 complexes and cohesin in replicatively aging cells. (A) Western blot of Sir2 protein levels in young and aged cells. Vma2 serves as a loading control. **(B)** Depiction of limiting Sir2 shared between the SIR and RENT complexes. **(C)** Western blot of Sir4 proteins in young and aged cells. **(D)** Western blot of Sir3 in young and aged cells. *(E)* Western blot of 13x-Myc tagged Net1 in young and aged cells. **(F)** Western blot of Mcd1-13xMyc in young and aged cells. **(G)** ChIP-qPCR of Mcd1-13xMyc in young and aged cells normalized to background signal at an intergenic site near *PDC1*. **(H)** ChIP-qPCR of Sir4-13xMyc in young and aged cells normalized to the intergenic *PDC1* site. Bud scar counts indicate the average for each enriched population used for the western blotting. Qty indicates the mean western signal of each protein in aged cells relative to the signal in young cells, which is set at 1.0 (n=3 biological replicates). Standard errors are provided in Supplementary Fig 1B.

Fig 3. Sister chromatid cohesion is weakened in old yeast cells. (A) Representative control images of arm cohesion in an *mcd1-1* mutant at permissive (25°C) and non-permissive (37°C) temperatures. **(B)** Quantification of cohesion maintenance (1-dot) or loss (2-dots) from 100 cells. **(C)** Representative images of young (log-phase) or aged cells arrested with nocodazole (Nz) and monitored for *CENIV* arm cohesion at the *LYS4* locus. **(D)** Images of cohesion at the *CEN4* locus in nocodazole-arrested young and aged cells. **(E)** Images of centromeric (*CEN*4) cohesion in young and aged cells not treated with Nz. **(F)** Quantifying cohesion loss (2-dots) young cells or aged cells with at least 5 bud scars (100 cells of each population). *$p<0.05$, two-tailed Fischer's exact test.

Fig 4. Chromosomal instability during replicative aging is linked to the rDNA. (A) Schematic of artificial chromosome loss assay for ½ sectored colonies. **(B)** Quantification of

919 sectoring frequency in young or aged WT, *sir2*Δ, *hst1*Δ, and *sir2*Δ *hst1*Δ strains. *HMR* or *FOB1*
920 were also deleted where indicated. Approximately 10,000 colonies were analyzed for each strain,
921 in several biological replicates. *p<0.05, two-tailed student t-test. **(C)** Iteratively corrected (IC)
922 and read-normalized heatmap of ChrXII Hi-C data at 10 kb resolution revealing a driving
923 interaction between *CEN12* (bin 15) and unique sequence adjacent to the rDNA (bin 45). **(D)**
924 Observed/expected statistical heatmap of ChrXII Hi-C data at 10 kb resolution using HOMER.
925 Yellow bracket indicates a putative loop structure between bins 15 and 45. **(E)** IC/read-
926 normalized Hi-C heatmap of chromosomes XI, XII, and XIII showing centromere clustering.
927 Yellow arrows indicate examples of centromere alignment with *CEN12*.

928 **Fig 5. Galactose induces CIN and shortens yeast RLS. (A)** Representative images of
929 chromosome loss (sectoring) for WT (YPH278) cells grown continuously in 2% glucose,
930 galactose, or raffinose. **(B)** Quantification of half-sector colonies for WT (YPH278) cells grown
931 on each carbon source. *p<0.01, two-tailed student t-test. **(C)** RLS assay of YPH278 cells (n=64)
932 growing on rich YEP agar plates containing either 2% glucose, galactose, or raffinose. **(D)** RLS
933 of WT (BY4741) cells (n=32) growing on 2% glucose, galactose, or raffinose.

934 **Fig 6. Modulation of RLS by manipulating *MCD1* and *SIR2* expression levels. (A)** RLS
935 assays of WT (*MCD1*$^{+}$) and *mcd1L12STOP* strains containing an integrated empty tet^{on}
936 expression vector or the same vector overexpressing *MCD1* (n=96 cells each strain). **(B)** RLS
937 assay of WT and *mcd1L12STOP* strains containing an integrated empty pRS306 vector or the
938 *SIR2* vector, pJSB186 (n=40 cells each). **(C)** RLS assay showing *MCD1* overexpression does not
939 rescue the short RLS of a *sir2Δhst1Δ* mutant. **(D)** rDNA recombination (marker loss) assay with
940 a strain bearing *ADE2* within the rDNA array. Either an empty tet^{on} vector (pRF10) or an *MCD1*

overexpressing version (pRF11) were integrated at the *leu2Δ1* locus of WT or *sir2*Δ versions of W303AR (* p<0.05, two-tailed t-test).

Fig 7. CR effects are upstream of Sir2 and Mcd1 function in old cells. **(A)** RLS assay of WT (JH5275b) and *mcd1L12STOP* (JH5276b) strains under normal 2% glucose and CR (0.5% glucose) conditions (n=32 cells). **(B)** Western blot of Mcd1-13xMyc levels in young and aged cells of the MEP strain RF10. Cultures were grown in YEP media containing either 2% or 0.5% glucose. **(C)** Chromosome loss (sectoring) assay showing reduced sectoring in WT (YPH278), *sir2*Δ (RF32), *hst1*Δ (RF33), and *sir2*Δ *hst1*Δ (RF43) strains when grown in media containing 0.5% glucose compared to 2%. * p<0.05, two-tailed t-test. **(D)** RLS assay of WT and *sir2Δhst1Δ* mutant strains under normal and CR conditions. (n=32 cells).

Fig 8. Model of residual cohesin redistribution from rDNA to centromeres in aging yeast cells. Centromeres of all 16 chromosomes cluster, and the rDNA remains isolated. The rDNA may also contact the centromeres during anaphase, which could impact the fidelity of chromosome segregation or promote recombination between the rDNA and other chromosomes. Cohesin and Sir2-containing complexes are depleted in cells, but the remaining cohesin complex preferentially associates with centromeres in a futile attempt to maintain sister chromatid cohesion.

Supporting Figure and Table Captions

S1 Fig. Detailed western blot and bud scar count quantification. (A) Bar graph showing average bud scar counts from young and aged cell populations used for western blotting. **(B)**

962 Detailed bud scar counts and western blot quantitation from the triplicate biological samples. **(C)**
963 Representative image of an enriched old cell population from the third Lrs4-13xMyc biological
964 replicate. Inset image allows counting of individual bud scars.

965 **S2 Fig. Western blots of additionally tested proteins from young and aged cells. (A)** A
966 13xMyc-tagged version of the Sir2 paralog, Hst1, is also depleted in aged cells. Hst1 is in a
967 complex with Sum1 and Rfm1. **(B)** The Myc-tagged Smc1 subunit of cohesin is depleted in aged
968 cells to similar levels as Mcd1. The yeast cohesin complex consists of Smc1, Smc3, Mcd1, and
969 Irr1. Smc1 and Smc3 form the coiled-coil loop structure. **(C)** A 13x-Myc tagged version of the
970 cohesin loading complex subunit, Scc2, also decreases in old cells. The cohesin loading complex
971 consists of Scc2 and Scc4.

972 **S3 Fig. RLS of the cohesion visualization strains is normal and unaffected by position of**
973 **the lacO array.** Strain 3349-1B contains a lacO array at the *LYS4* locus on Chr. IV and is used
974 as a proxy for arm cohesion, while strain 3460-2A is used to monitor centromeric cohesion 10 kb
975 away from the *CEN4* locus.

976 **S4 Fig. Confirmation of doxycycline-induced *MCD1* overexpression in WT and**
977 **mcd1L12STOP strains.** RT-qPCR of *MCD1* transcript levels relative to actin transcript levels
978 were quantified from the empty vector strains (RF146 and RF147) or the *MCD1* overexperssion
979 strains RF179 and RF180. Total RNA was isolated following 6 hours doxycycline induction
980 during log-phase growth.

981

982 **S1 Table. Yeast Strains.** This table lists each *Saccharomyces cerevisiae* strain used in the study,

983 along with its genotype and source.

984 **S2 Table. Oligonucleotides used in the study.**

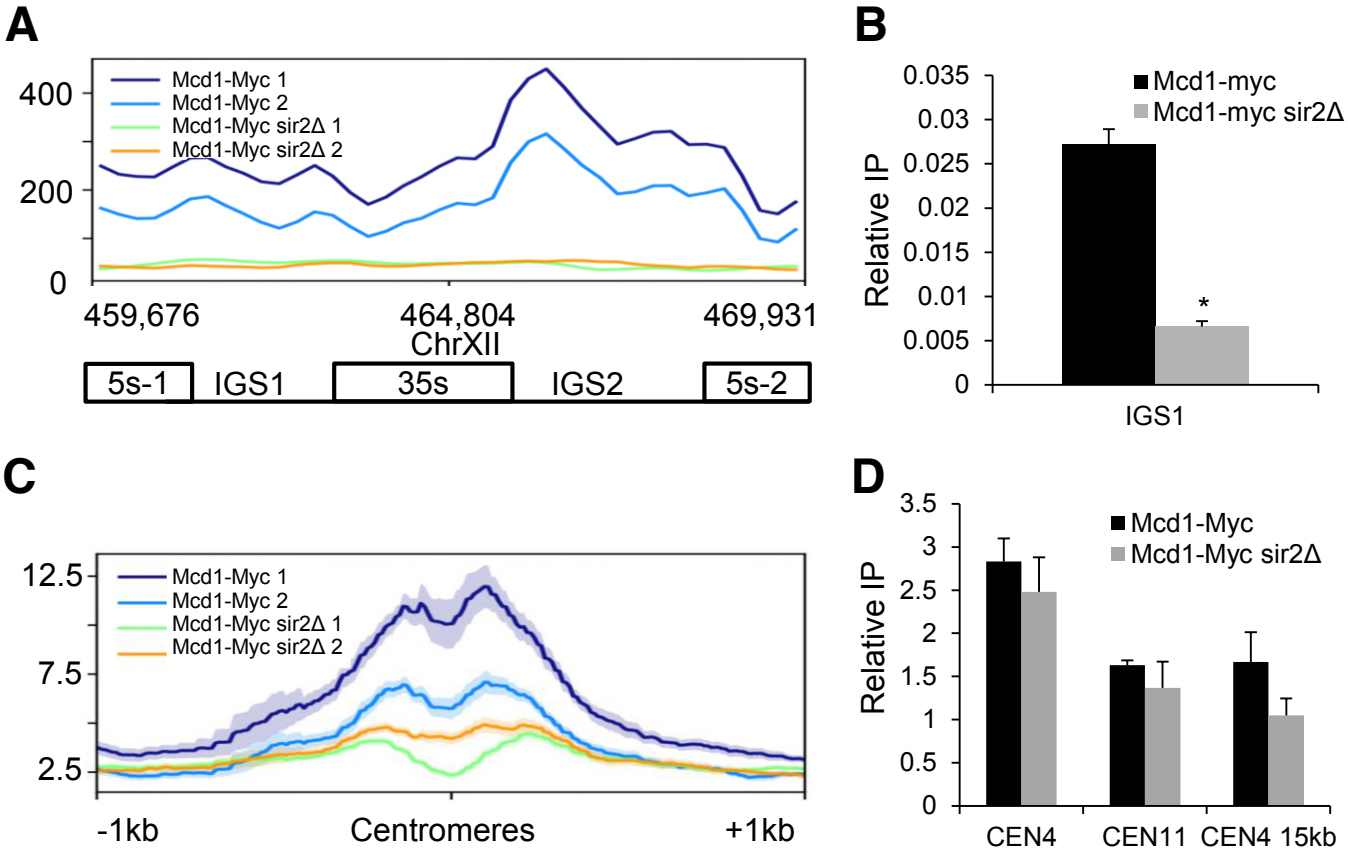
A
Mcd1-Myc 1
Mcd1-Myc 2
Mcd1-Myc sir2Δ 1
Mcd1-Myc sir2Δ 2
400
200
0
459,676
464,804
ChrXII
469,931
5s-1
IGS1
35s
IGS2
5s-2
B
Mcd1-myc
Mcd1-myc sir2Δ
Relative IP
0.035
0.03
0.025
0.02
0.015
0.01
0.005
0
*
IGS1
C
Mcd1-Myc 1
Mcd1-Myc 2
Mcd1-Myc sir2Δ 1
Mcd1-Myc sir2Δ 2
12.5
7.5
2.5
-1kb
Centromeres
+1kb
D
Mcd1-Myc
Mcd1-Myc sir2Δ
Relative IP
3.5
3
2.5
2
1.5
1
0.5
0
CEN4
CEN11
CEN4 15kb

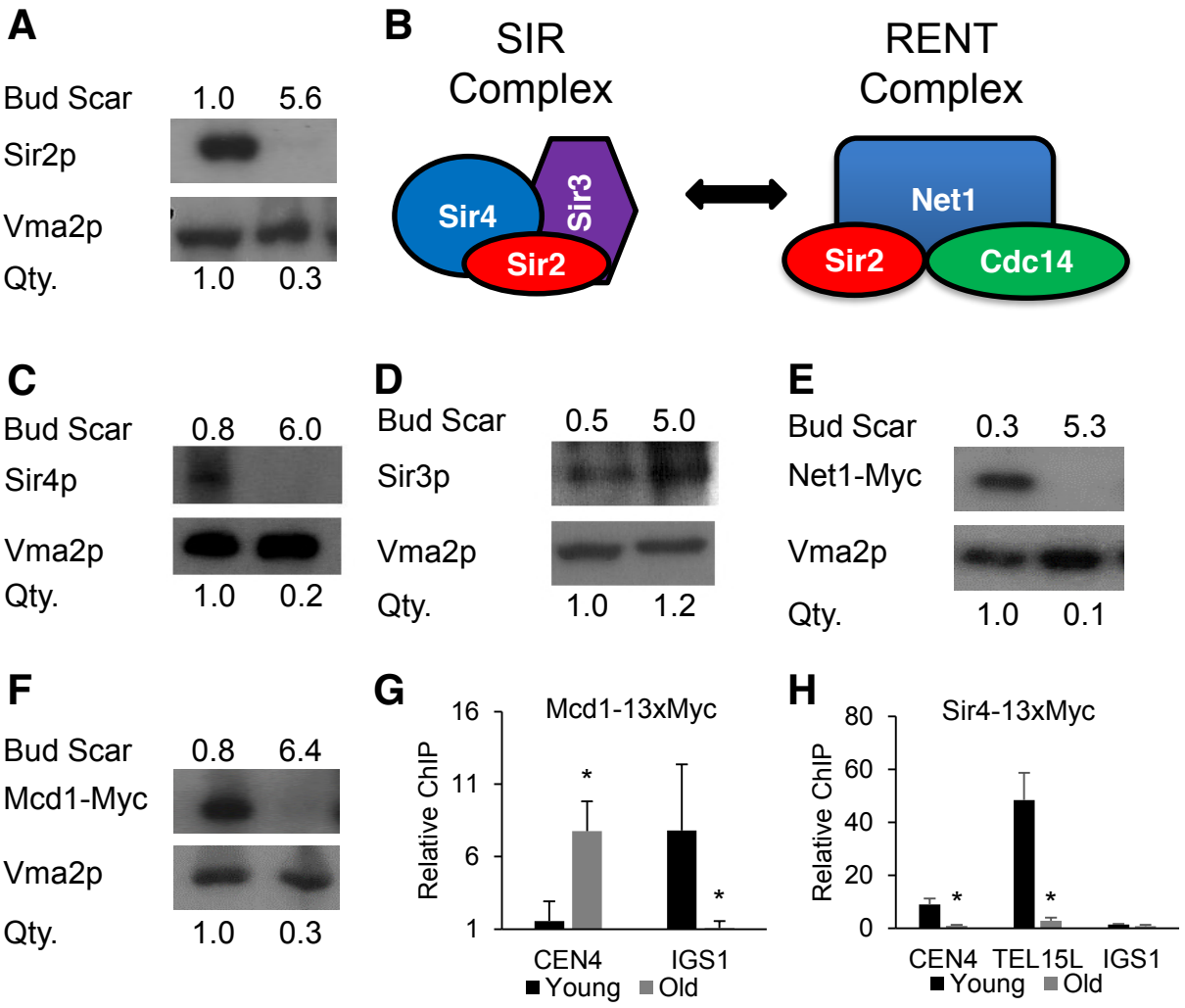
A
Bud Scar 1.0 5.6
Sir2p
Vma2p
Qty. 1.0 0.3
B
SIR Complex
RENT Complex
Sir4
Sir3
Sir2
Net1
Sir2
Cdc14
C
Bud Scar 0.8 6.0
Sir4p
Vma2p
Qty. 1.0 0.2
D
Bud Scar 0.5 5.0
Sir3p
Vma2p
Qty. 1.0 1.2
E
Bud Scar 0.3 5.3
Net1-Myc
Vma2p
Qty. 1.0 0.1
F
Bud Scar 0.8 6.4
Mcd1-Myc
Vma2p
Qty. 1.0 0.3
G
Mcd1-13xMyc
Relative ChIP
16
11
6
1
CEN4
IGS1
Young
Old
H
Sir4-13xMyc
Relative ChIP
80
60
40
20
0
CEN4
TEL15L
IGS1
Young
Old

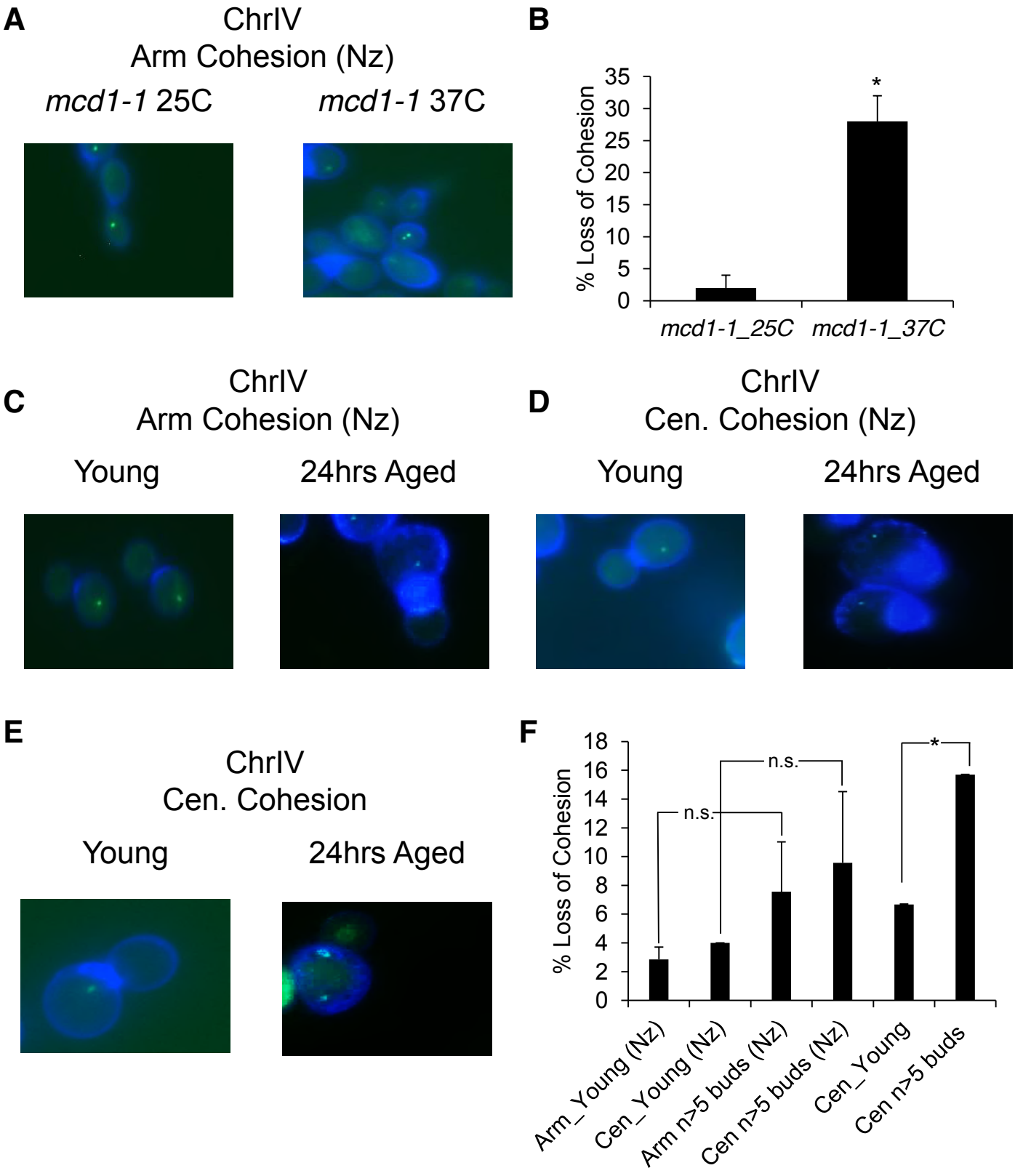
A
ChrIV
Arm Cohesion (Nz)
mcd1-1 25C
mcd1-1 37C
B
% Loss of Cohesion
35
30
25
20
15
10
5
0
*
mcd1-1_25C
mcd1-1_37C
C
ChrIV
Arm Cohesion (Nz)
Young
24hrs Aged
D
ChrIV
Cen. Cohesion (Nz)
Young
24hrs Aged
E
ChrIV
Cen. Cohesion
Young
24hrs Aged
F
% Loss of Cohesion
18
16
14
12
10
8
6
4
2
0
n.s.
n.s.
*
Arm_Young (Nz)
Cen_Young (Nz)
Arm n>5 buds (Nz)
Cen n>5 buds (Nz)
Cen_Young
Cen n>5 buds

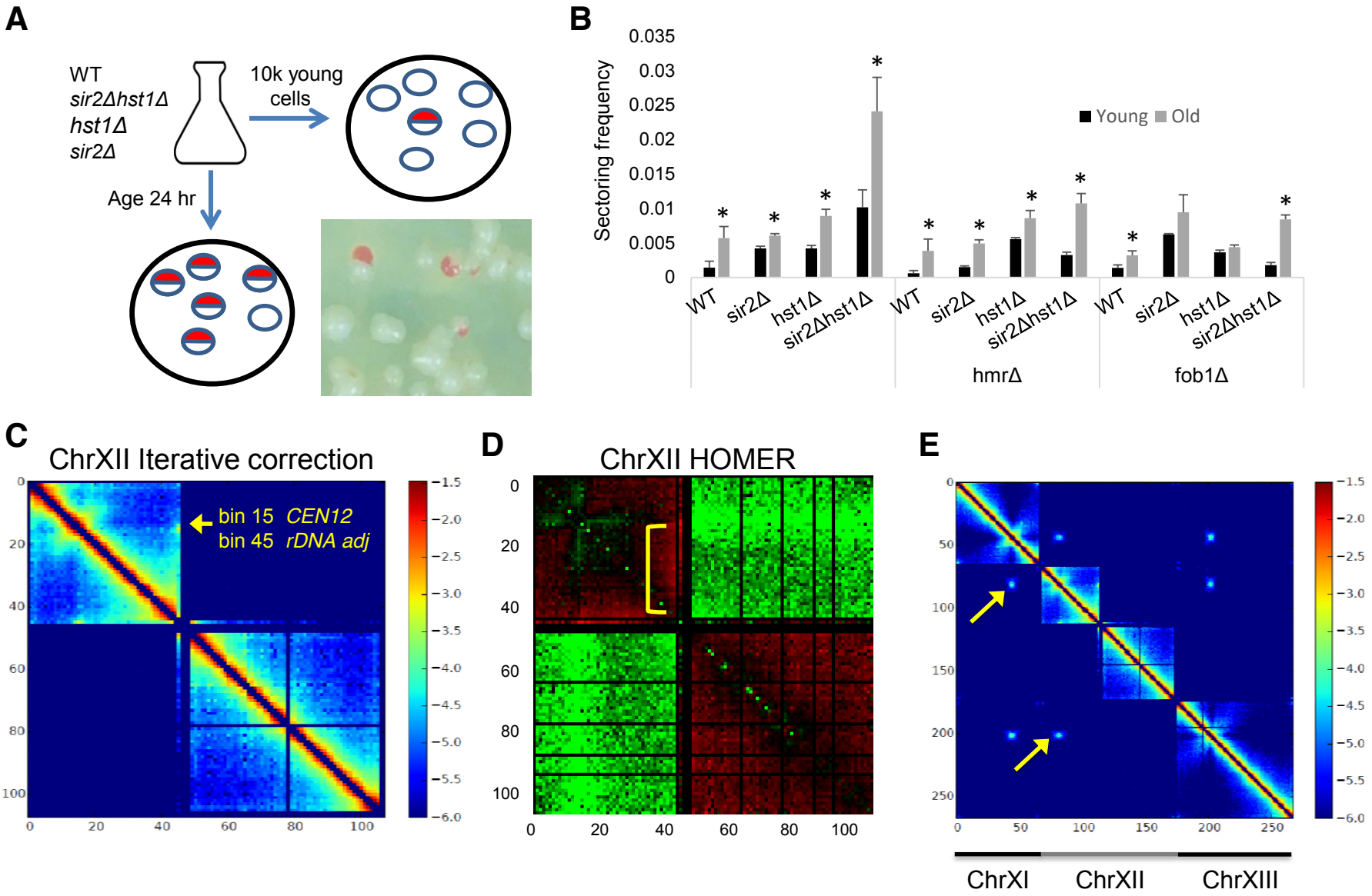
A
WT
sir2Δhst1Δ
hst1Δ
sir2Δ
10k young cells
Age 24 hr
B
Sectoring frequency
0.035
0.03
0.025
0.02
0.015
0.01
0.005
0
Young
Old
WT
sir2Δ
hst1Δ
sir2Δhst1Δ
hmrΔ
fob1Δ
C
ChrXII Iterative correction
bin 15 CEN12
bin 45 rDNA adj
D
ChrXII HOMER
E
ChrXI
ChrXII
ChrXIII

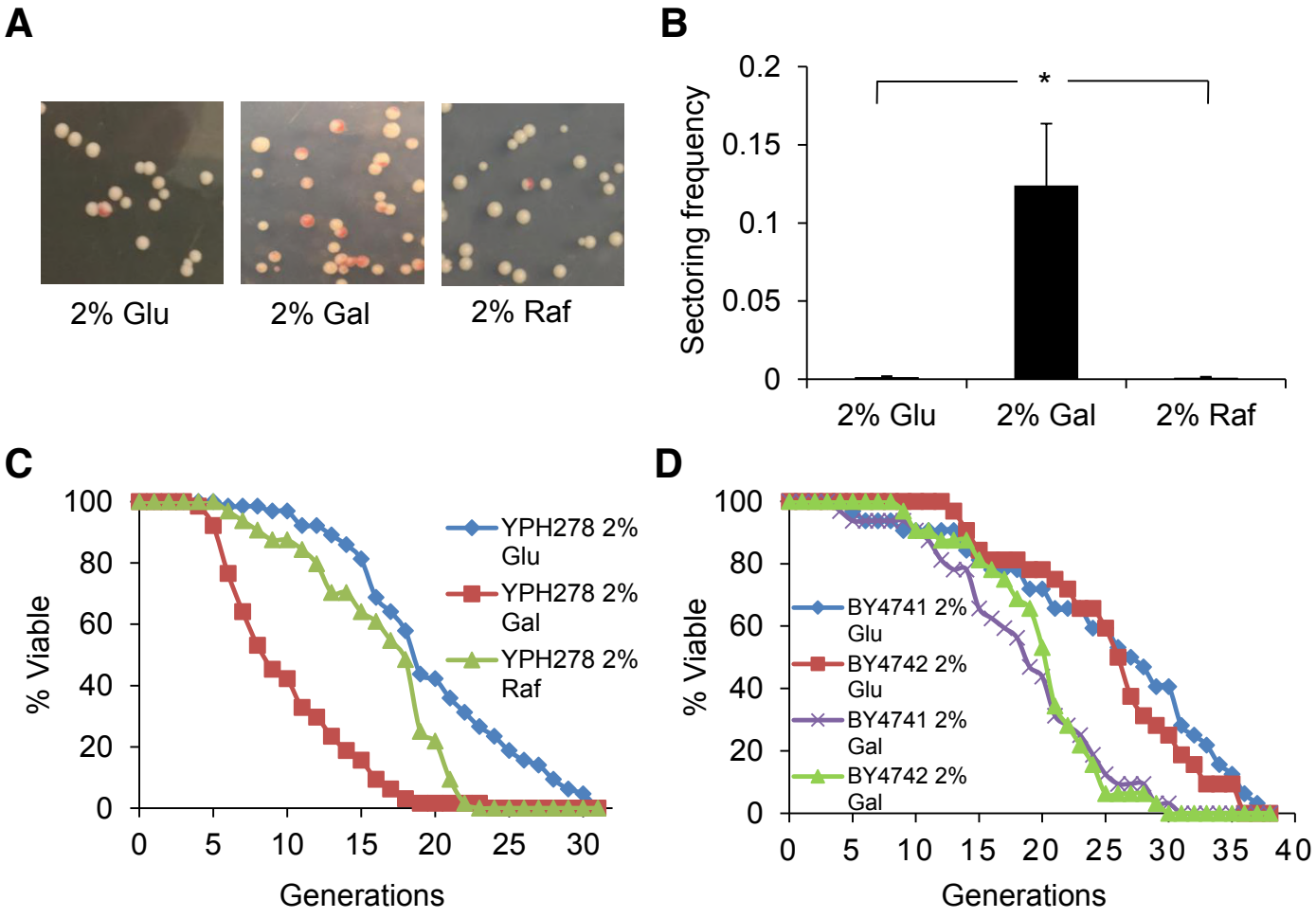
A
2% Glu
2% Gal
2% Raf
B
Sectoring frequency
0.2
0.15
0.1
0.05
0
*
2% Glu
2% Gal
2% Raf
C
% Viable
100
80
60
40
20
0
0
5
10
15
20
25
30
Generations
YPH278 2% Glu
YPH278 2% Gal
YPH278 2% Raf
D
% Viable
100
80
60
40
20
0
0
5
10
15
20
25
30
35
40
Generations
BY4741 2% Glu
BY4742 2% Glu
BY4741 2% Gal
BY4742 2% Gal

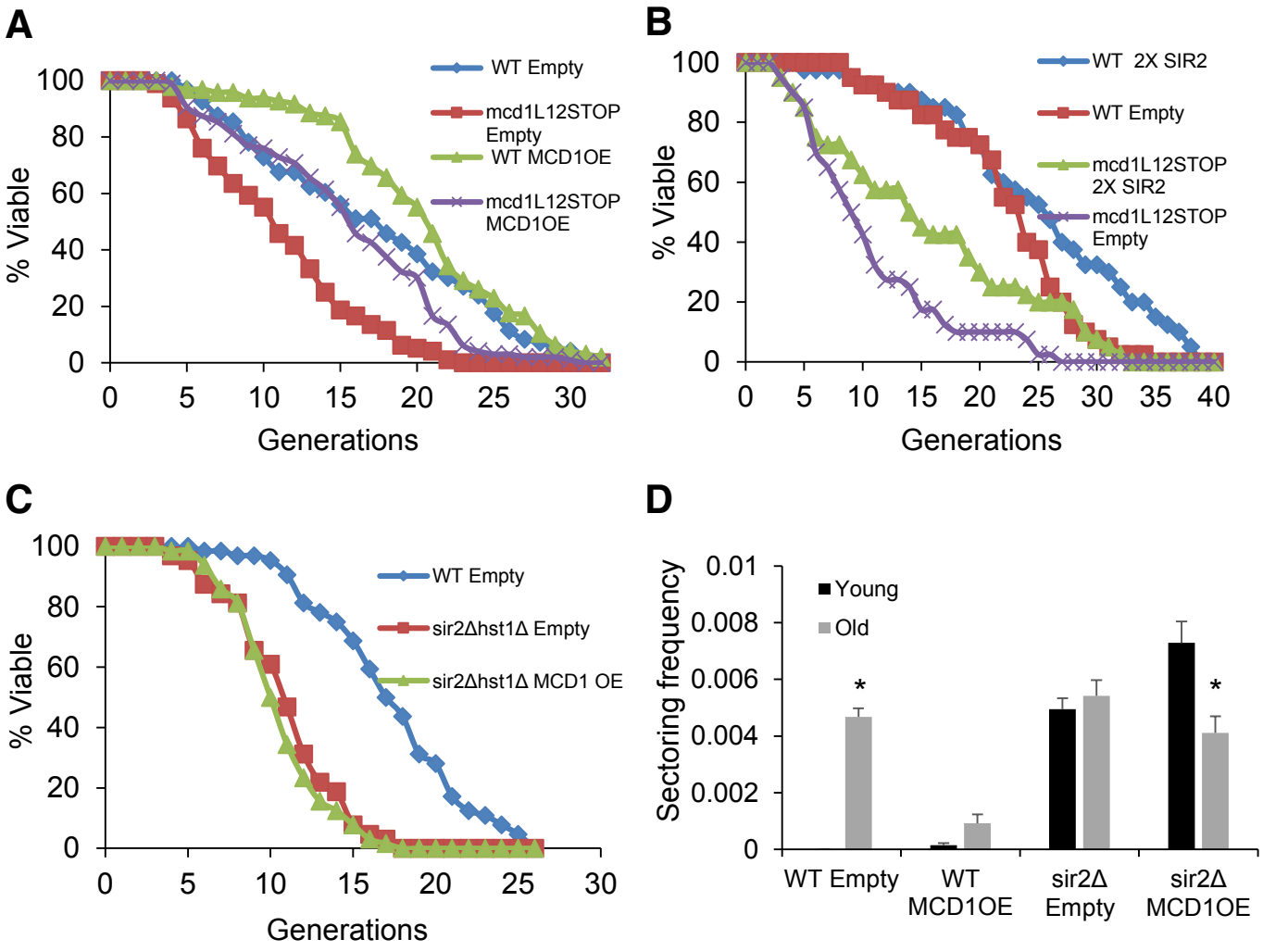
A
100
80
60
40
20
0
% Viable
0
5
10
15
20
25
30
Generations
WT Empty
mcd1L12STOP Empty
WT MCD1OE
mcd1L12STOP MCD1OE
B
100
80
60
40
20
0
% Viable
0
5
10
15
20
25
30
35
40
Generations
WT 2X SIR2
WT Empty
mcd1L12STOP 2X SIR2
mcd1L12STOP Empty
C
100
80
60
40
20
0
% Viable
0
5
10
15
20
25
30
Generations
WT Empty
sir2Δhst1Δ Empty
sir2Δhst1Δ MCD1 OE
D
Sectoring frequency
0.01
0.008
0.006
0.004
0.002
0
Young
Old
*
*
WT Empty
WT MCD1OE
sir2Δ Empty
sir2Δ MCD1OE

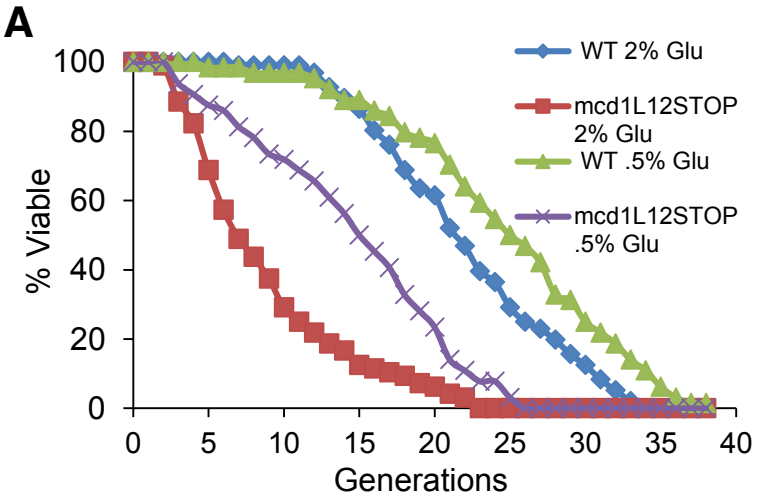
A
100
80
60
40
20
0
% Viable
0
5
10
15
20
25
30
35
40
Generations
WT 2% Glu
mcd1L12STOP 2% Glu
WT .5% Glu
mcd1L12STOP .5% Glu

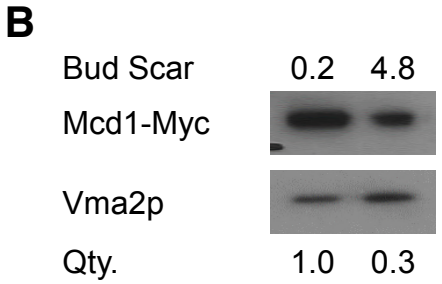
B
Bud Scar
0.2
4.8
Mcd1-Myc
Vma2p
Qty.
1.0
0.3

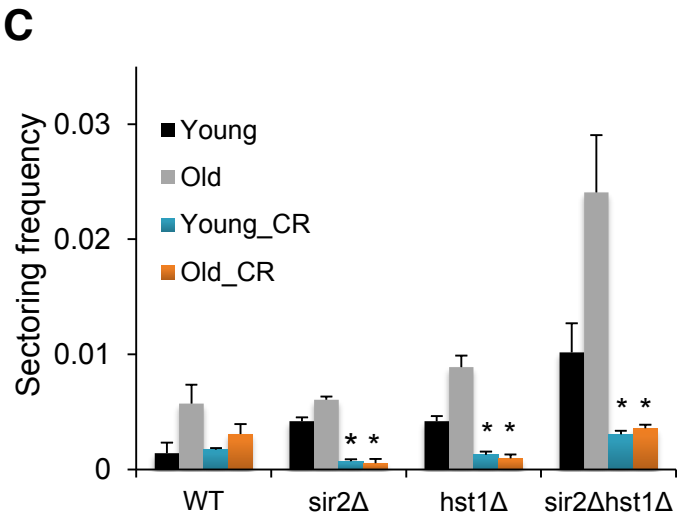
C
Sectoring frequency
0.03
0.02
0.01
0
Young
Old
Young_CR
Old_CR
* *
* *
* *
WT
sir2Δ
hst1Δ
sir2Δhst1Δ

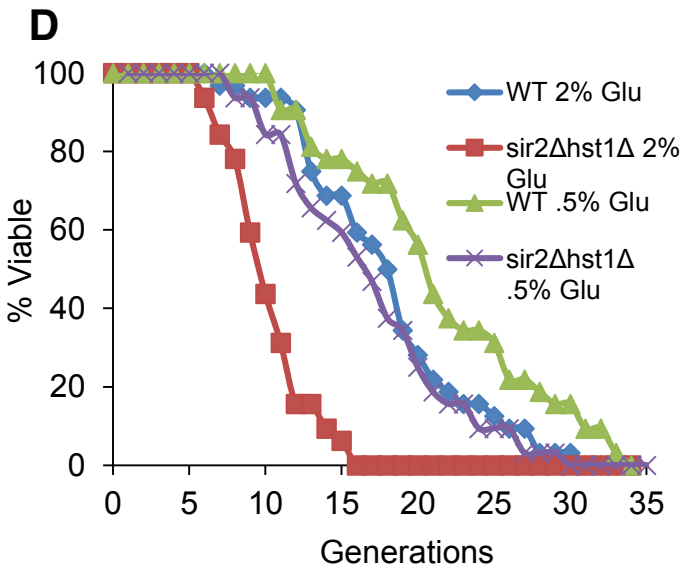
D
100
80
60
40
20
0
% Viable
0
5
10
15
20
25
30
35
Generations
WT 2% Glu
sir2Δhst1Δ 2% Glu
WT .5% Glu
sir2Δhst1Δ .5% Glu

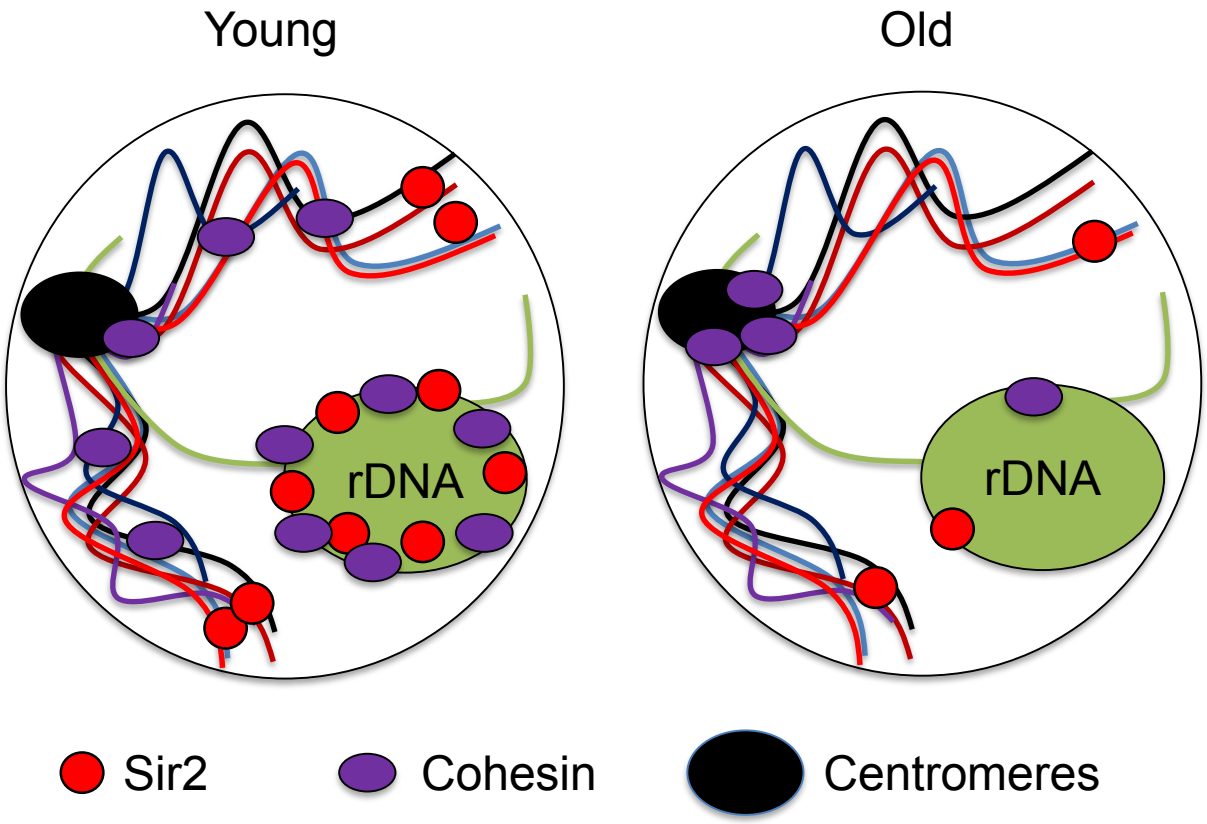
Young
Old
rDNA
rDNA
Sir2
Cohesin
Centromeres